V. THEORETICAL PHYSICS

OVERVIEW

Our research addresses the five key questions that comprise the Nation's scientific agenda. We place heavy emphasis on the prediction of phenomena accessible at Argonne's ATLAS facility, at JLab, and at other laboratories around the world; and particularly on anticipating and planning for RIA. One focus is the application of quantum chromodynamics (QCD) to the structure of light- and heavy-hadrons: in vacuum, as relevant to programs such as those pursued at JLab; and in-medium, as appropriate to the early universe, compact astrophysical objects, and the RHIC program. The interactions between light hadrons are studied through the development of reaction theories that exploit modern ideas of hadron structure and which are then used to predict the outcomes of experiments at, *e.g.*, JLab, MIT-Bates and Mainz. The structure and stability of atomic nuclei are explored in *ab-initio* many-body calculations based on the realistic two- and three-nucleon potentials we have constructed. These potentials give excellent fits to nucleon-nucleon elastic scattering data and the properties of light nuclei. In addition, quantum Monte-Carlo methods are being used to compute scattering phase shifts, transition amplitudes, and a variety of electroweak reactions important to astrophysics. Our nuclear structure and reaction program includes: coupled-channels calculations of heavy-ion reactions near the Coulomb barrier; calculations of observables in breakup reactions of nuclei far from stability, the determination of radiative capture rates from Coulomb dissociation experiments, and studies of high-spin deformation and the structure of the heaviest elements. Our programs provide much of the scientific basis for the drive to physics with rare isotopes. Additional research in the Group focuses on atomic physics, neutron physics, fundamental quantum mechanics and quantum computing. The pioneering development and use of massively parallel numerical simulations using hardware at Argonne and elsewhere is a major component of the Group's research.

A. NUCLEAR DYNAMICS WITH SUBNUCLEONIC DEGREES OF FREEDOM

The objective of this research program is to investigate the role of: quark-gluon degrees of freedom in hadron structure and interactions, and in nuclear dynamics; the development and application of reaction theories for use in exploring hadron structure using the data from meson and nucleon-resonance production experiments at modern experimental facilities; and to investigate relations of Poincaré covariant dynamics specified by mass operators to complementary dynamics specified by Green functions.

At the level of quark-gluon degrees of freedom, the Dyson-Schwinger equations (DSEs) provide a Poincaré covariant, nonperturbative method for studying QCD in the continuum. A hallmark of present-day DSE applications in hadron physics is the existence of a symmetry preserving truncation that enables the simultaneous exploration of phenomena such as: confinement, dynamical chiral symmetry breaking, and bound state structure and interactions. In addition the DSEs provide a generating tool for perturbation theory and hence yield model-independent results for the ultraviolet behavior of strong interaction observables. This means that model studies facilitate the use of physical processes to constrain the long-range behavior of the interaction between light-quarks in QCD, which is poorly understood and whose elucidation is a key goal of modern experimental programs. The last year saw numerous successful applications. For example, we demonstrated that the leading-order (rainbow-ladder) term in the DSE truncation scheme, when consistently implemented, is necessary and sufficient to express the Abelian anomaly. We capitalized on this to show that even though excited state pseudoscalar mesons decouple from the axial-vector current in the chiral limit, they nevertheless couple to two photons. It follows that the Primakov process may be used as a tool for their production and study. Furthermore, we employed a Poincaré covariant Faddeev equation to obtain masses and amplitudes for the nucleon and Δ. We subsequently formulated a nucleon-photon vertex, which automatically ensures the vector Ward-Takahashi identity is fulfilled for on-shell nucleons described by the calculated Faddeev amplitudes. This guarantees current conservation. These elements are sufficient for a calculation of the quark contribution to the nucleons' electromagnetic form factors. Our results provide a straightforward explanation of contemporary JLab data on the ratio of the proton's electric and magnetic form factors. Poincaré covariance and pion cloud effects are keystones of this understanding.

At the level of meson and baryon degrees of freedom, we are continuing our effort to develop dynamical models for use in the study of few-GeV electromagnetic meson production reactions. Our objective is an interpretation of the extensive data from JLab in terms of the quark-gluon substructure of nucleon resonances (N^*) as predicted by QCD-based hadron models and simulations of lattice-QCD. In the past year, we have extended our model for pion electroproduction in the Δ region to include neutral current contributions so as to examine local Quark-Hadron Duality in neutrino-induced reactions and determine how the axial N-Δ form factor my be determined from a parity violating asymmetry in inclusive $N(\vec{e},e')$ reactions. We have completed the development of a coupled-channel dynamical model and started to analyze JLab data on two-pion and kaon production. We have completed our study of production mechanisms for the recently observed, narrow-width Θ^+ resonance and found that JLab's data can be fitted by a model consisting of the so-called Drell diagrams ($K\overline{K}$ production through

intermediate vector and tensor meson photoproduction) and mechanisms involving nucleon resonances. An Eikonal model was developed for investigating ρ-meson photoproduction on nuclei. We aim here to analyze JLab data obtained by Argonne's Medium Energy Group to explore Color Transparency issues and address a long-standing question regarding medium effects on di-lepton production in relativistic heavy-ion reactions.

Relativistic quantum dynamics requires a unitary representation of space-time symmetries (Poincaré group) and localization of states, such that states localized in relatively space-like regions are causally independent. We have recently focused on the application and elucidation of complementary mathematical representations of hadron phenomena.

a.1. Aspects and Consequences of a Dressed-Quark-Gluon Vertex (M. S. Bhagwat,* A. Höll, A. Krassnigg, C. D. Roberts, and P. C. Tandy*)

This dressed-quark-gluon vertex is a Schwinger function whose properties are a key to unlocking the nature of light-quark confinement. We explored features of this vertex and their role in the gap and Bethe-Salpeter equations. It became apparent that quenched lattice data indicate the existence of net attraction in the color-octet projection of the quark-antiquark scattering kernel. We saw that this attraction affects the uniformity with which solutions of truncated equations converge pointwise to solutions of the complete gap and vertex equations. We observed that for current-quark masses less than the scale set by dynamical chiral symmetry breaking, the dependence of the dressed-quark-gluon vertex on the current-quark mass is weak and, using a chiral susceptibility, argued that a linear extrapolation to the chiral limit of the results of lattice-QCD simulations of the dressed-quark propagator is inaccurate.

Our analysis employed a vertex model whose diagrammatic content is explicitly enumerable. That enabled the systematic construction of a vertex-consistent Bethe-Salpeter kernel and thereby an exploration of the consequences for the strong interaction spectrum of attraction in the color-octet channel. We found that with rising current-quark mass the rainbow-ladder truncation provides an increasingly accurate estimate of a bound state's mass. Moreover, the calculated splitting between vector and pseudoscalar meson masses vanishes as the current-quark mass increases, which argues for the mass of the pseudoscalar partner of the Y(1S) to be above 9.4 GeV.

Moreover, our calculations showed that the absence of color-antitriplet diquarks from the strong interaction spectrum is contingent upon the net amount of attraction in the octet projected quark-antiquark scattering kernel. While there is a window within which diquarks appear, the amount of attraction suggested by lattice results is outside this domain.

An article describing this work was published[1] and another submitted.[2]

*Kent State University.

[1]M. S. Bhagwat, A. Höll, A. Krassnigg, C. D. Roberts, and P. C. Tandy, Phys. Rev. C **70**, 035205 (2004).
[2]A. Höll, A. Krassnigg, and C. D. Roberts, Nucl. Phys. **B141**, 47 (2005).

a.2. Pseudoscalar Meson Radial Excitations (A. Höll, A. Krassnigg, and C. D. Roberts)

The known meson spectrum contains three pseudoscalars [I^G (J^{PC}) = 1^- (0^{-+})], all with masses below *2* GeV: *π(140)*; *π(1300)*; and *π(1800)*. The lightest of these, the pion [*π(140)*], is much studied and well understood as QCD's Goldstone mode. It is the key degree of freedom in chiral effective theories, and a veracious explanation of its properties requires an approach to possess a valid realization of chiral symmetry and its dynamical breaking. The *π(1300)* is likely the first radial excitation of *π(140)* and while the *π(1800)* may be the second radial excitation, it could also be a hybrid; *i.e.*, a state with nontrivial constituent-glue-like content. A

hallmark in the contemporary use of Dyson-Schwinger equations is the existence of a nonperturbative, symmetry preserving truncation scheme. We used this scheme to prove that of all pseudoscalar mesons supported by QCD, only the Goldstone modes possess a nonzero leptonic decay constant in the chiral limit when chiral symmetry is dynamically broken. The decay constants of all other pseudoscalar mesons vanish, whether they are radial excitations or hybrids; viz., $f(\pi_n) = 0$ for all $n \geq 1$. This means that in the chiral limit every pseudoscalar meson is blind to the weak interaction except the $\pi(140)$. This exact result places a very tight constraint on all models and nonperturbative methods in their application to hadron spectroscopy and interactions, particularly in connection with the search for exotic and hybrid states in the *1-2* GeV range.

We illustrated these features and aspects of their impact on the meson spectrum using a model of the kernels in the gap and Bethe-Salpeter equations. This work provides the first Poincaré covariant and symmetry preserving analysis of meson excited states. Moreover, it shows that at realistic current-quark masses the leptonic decay constant of the first radial excitation is two orders of magnitude smaller than that of the $\pi(140)$; and gives the first direct indication that when the current-quark mass is nonzero the leptonic decay constants of mesons on the pseudoscalar trajectory alternate in sign; viz., the decay constants of the ground state and the 2nd, 4th, etc. heaviest states are positive, while those of the 1st, 3rd, etc. are negative. *A posteriori* it is apparent that this outcome is necessary to ensure that the spectral density in the 1^{++} channel is non-negative. Nevertheless, the result was not anticipated nor reported previously.

The model was also used to predict: $f(\eta_c) = 0.233$GeV and $m(\eta_c) = 3.42$GeV. In addition, studies were made within this framework that provide support for an interpretation of $\eta(1295)$ and $\acute{\eta}(1470)$ as radial excitations of $\eta(548)$ and $\acute{\eta}(958)$, respectively; and $K(1460)$ as the first radial excitation of the kaon.

Articles describing this work were published.[1,2]

[1] A. Höll, A. Krassnigg, and C. D. Roberts, Phys. Rev. C **70**, 042203(R) (2004).
[2] A. Höll, A. Krassnigg, C. D. Roberts, and S. V. Wright, Int. J. Mod. Phys. A **20**, 1778 (2005).

a.3. Nucleon Electromagnetic Form Factors (R. Alkofer,* A. Höll, M. Kloker,* A. Krassnigg, C. D. Roberts, and S. V. Wright)

Modern, high-luminosity experimental facilities that employ large momentum transfer reactions are providing remarkable and intriguing new information on nucleon structure. At values of momentum transfer, $Q^2 > M^2$, where M is the nucleon's mass, a veracious understanding of these data requires a Poincaré covariant description of the nucleon. We employed a Poincaré covariant Faddeev equation that describes baryons as composites of confined-quarks and -diquarks, and solved this equation to obtain masses and amplitudes for the nucleon and Delta. Two parameters appear in the model Faddeev equation: masses of the scalar and axial-vector diquark correlations. They were fixed by fitting stipulated masses of the baryons. We interpreted the masses and Faddeev amplitudes thus obtained as representing properties of the baryons' *quark core* and argued that this should be augmented in a consistent fashion by chiral-loop corrections.

We described the formulation of a nucleon-photon vertex, which automatically ensures the vector Ward-Takahashi identity is fulfilled for on-shell nucleons described by the calculated Faddeev amplitudes. This guarantees current conservation. The vertex *Ansatz* involves three parameters. Two of these specify electromagnetic properties of axial-vector diquarks and a third measures the strength of electromagnetically induced axial-vector↔scalar-diquark transitions. These quantities are also properties of the nucleons' quark core.

These elements are sufficient for a calculation of the quark contribution to the nucleons' electromagnetic form factors. We explored a reasonable range of nucleon-photon-vertex parameter values and found that an accurate description of the nucleons' static properties was not possible with the core components alone. However, this mismatch with experiment was greatly reduced by the inclusion of chiral corrections. Since true pseudoscalar mesons are not pointlike their contribution to baryon form factors diminishes with increasing momentum transfer. Hence, experiments on nucleons involving $Q^2 > 2\text{GeV}^2$ probe properties of the Poincaré covariant quark core.

We calculated ratios of the proton's form factors. On the whole domain of nucleon-photon-vertex parameter values explored, the calculated behavior of $G_{Ep}(Q^2)/G_{Mp}(Q^2)$ for $Q^2 > 2\text{GeV}^2$ agrees with that inferred from contemporary polarization transfer data, and this ratio exhibits a zero at $Q^2 \approx 6.5\text{GeV}^2$. These features are evident in Fig. V-1. Moreover, there is evidence that

$$F_2(Q^2)/F_1(Q^2) \approx (\ln [Q^2/M^2])^2/Q^2 \text{ for } Q^2 > 6\text{GeV}^2.$$

Since the parameters in the nucleon-photon vertex do not influence these outcomes, we judge they are manifestations of features intrinsic to the nucleon's Faddeev amplitude. In the nucleon's rest frame, this amplitude corresponds to a relativistic wave function with *s*–, *p*– and even *d*–wave quark orbital angular momentum components.

Our study supports a view that baryons can realistically be seen as a dominant Poincaré covariant quark core, augmented by pseudoscalar meson cloud contributions that, *e.g.*, make a noticeable contribution to form factors for $Q^2 < 2\text{GeV}^2$. Since meson compositeness ensures that such contributions diminish with increasing Q^2, experiments at larger Q^2 serve as an instructive probe of correlations in baryon wave functions; *i.e.*, their Faddeev amplitudes. A good understanding of QCD's long-range dynamics is required in order to obtain a reliable quark-core wave function.

An article describing this work was published[2] and another submitted.[1]

---

*University of Tübingen, Germany.

[1]R. Alkofer, A. Höll, M. Kloker, A. Krassnigg, and C. D. Roberts, to appear in Few Body Systems.
[2]A. Höll, R. Alkofer, M. Kloker, A. Krassnigg, C. D. Roberts, and S. V. Wright, Nucl. Phys. **A755**, 298 (2005).

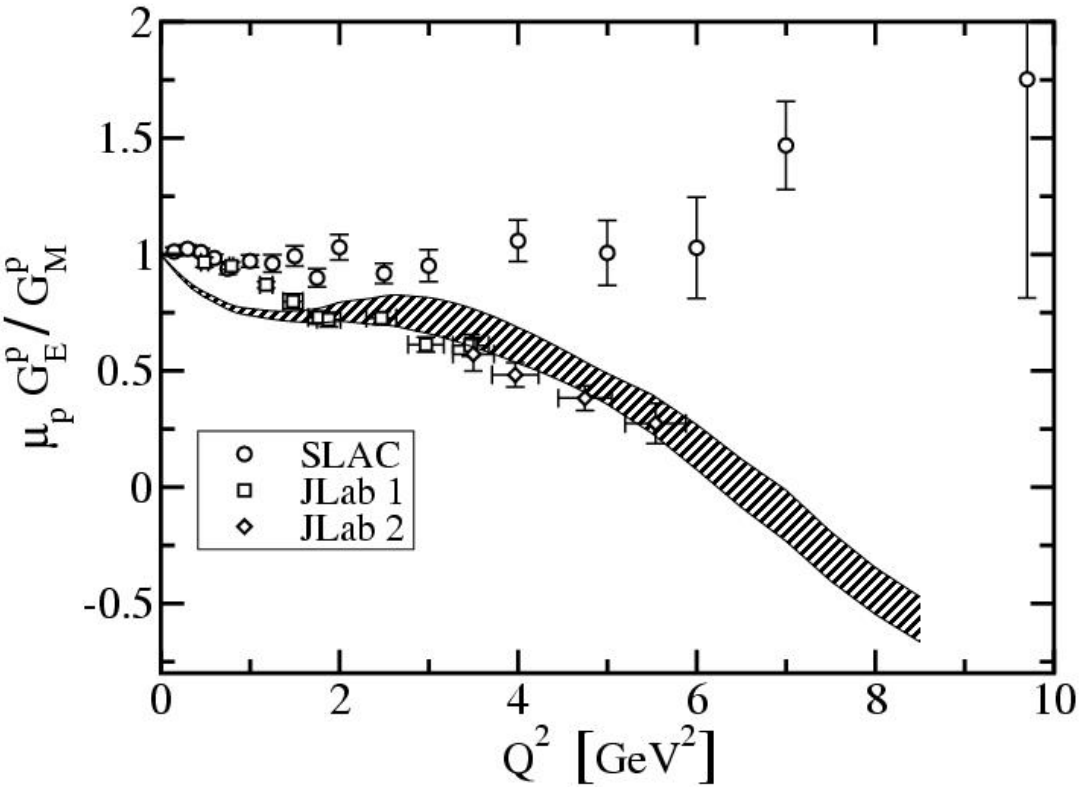

Fig. V-1. This result for the form factor ratios is taken from Ref. 2. Our calculation is the shaded band, whose extent marks the range of sensitivity to the three parameters that characterize our nucleon-photon current. The data are: SLAC – R. C. Walker et al., Phys. Rev. D ***49****, 5671 (1994); JLAB1 – M. K. Jones et al., Phys. Rev. Lett.* ***84****, 1398 (2000); and JLAB2 – O. Gayou et al., Phys. Rev. Lett.* ***88****, 092301 (2002).*

a.4. Electromagnetic Properties of Ground and Excited State Pseudoscalar Mesons

(A. Höll, A. Krassnigg, P. Maris,* C. D. Roberts, and S. V. Wright)

The strong interaction spectrum exhibits trajectories of mesons with the same spin+parity, J^P. One may distinguish between the states on these trajectories by introducing an integer label n, with $n=0$ denoting the lowest-mass state, $n = 1$ the next-lightest state, etc. The Bethe-Salpeter equation (BSE) yields the mass and amplitude of every bound state in a given channel specified by J^P. Hence it provides a practical tool for the Poincaré covariant study of mesons on these trajectories. A significant feature of such applications is the fact that at least one nonperturbative and symmetry preserving Dyson-Schwinger equation (DSE) truncation scheme exists. This supports the proof of exact results such as, *e.g.*, in the chiral limit excited state 0^- mesons do not couple to the axial-vector current; viz., $f(\pi_n) \equiv 0$ for all $n \geq 1$.

We demonstrated that the leading-order (rainbow-ladder) term in the DSE truncation scheme, when consistently implemented, is necessary and sufficient to express the Abelian anomaly. It can therefore be used to illustrate the anomaly's observable consequences. We capitalized on this to show that even though excited state pseudoscalar mesons decouple from the axial-vector current in the chiral limit, they nevertheless couple to two photons. It follows that the Primakov process, as employed for example in *PrimEx* at JLab, may be used as a tool for their production and study. We established in addition that the strength of the two-photon coupling is materially

affected by the continuum contribution to the Abelian anomaly.

A renormalization-group-improved rainbow-ladder truncation is guaranteed to express the one-loop renormalization group properties of QCD. We exploited this and thereby determined the leading power-law behavior of the $\gamma^*\ \pi_n\ \gamma^*$ transition form factor. When the current-quark mass is nonzero then this form factor behaves as $(4\pi^2/3)\ (f(\pi_n)/Q^2)$ at deep spacelike momenta. For all but the Goldstone mode this leading order contribution vanishes in the chiral limit. In that case, however, the form factor remains nonzero and the ultraviolet behaviour is $\approx (4\pi^2/3)\ (-\langle \bar{q}\, q\rangle/Q^4)$. These results are illustrated in Fig. V-2. Although only exposed starkly in the chiral limit for excited states, this subleading power-law contribution to the transition form factor is always present and in general its coefficient is not simply related to $f(\pi_n)$.

As one might rationally expect, the properties of excited ($n \geq 1$) states are sensitive to the pointwise behavior of what might be called the confinement potential between light-quarks. We illustrated this by laying out the evolution of the charge radii of the $n = 0,1$ pseudoscalar mesons. As it is shielded by Goldstone's theorem, the ground state's radius can be insensitive to details of the long-range part of the interaction. However, that is not true of $r(\pi_1)$, the radius of the first excited state, which is orthogonal to the vacuum. An increase in the length-scale that characterizes the range of the confining potential reduces $r(\pi_1)$. This result states that increasing the confinement force compresses the excited state: indeed, it is possible to obtain $r(\pi_1) < r(\pi_0)$. However, our current best estimate is $r(\pi_1) \approx 1.4\ r(\pi_1)$.

A detailed exploration of the properties of collections of mesons on particular J^P trajectories offers the hope of exposing features of the long-range part of the interaction between light-quarks. In principle, this interaction can be quite different to that between heavy-quarks. The pseudoscalar trajectory is of particular interest because its lowest mass entry is QCD's Goldstone mode. Chiral current conservation places constraints on some properties of every member of this trajectory, whose study may therefore provide information about the interplay between confinement and dynamical chiral symmetry breaking.

An article describing this work was published.[1]

---

*University of Pittsburgh.

[1]A. Höll, A. Krassnigg, P. Maris, C. D. Roberts, and S. V. Wright, Phys. Rev. C **71**, 065204 (2005).

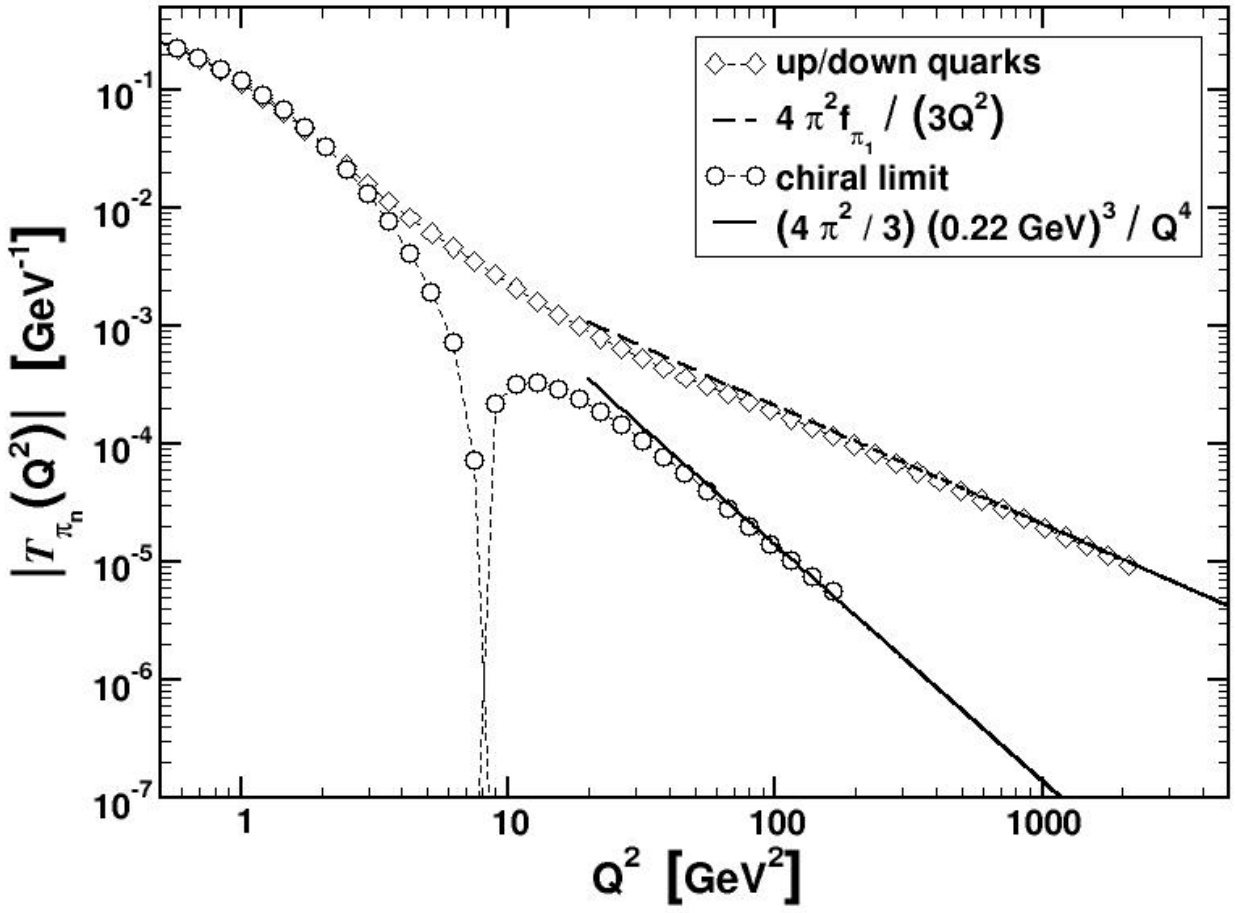

Fig. V-2. Large- Q^2 behavior of the $\gamma^* \pi_n \gamma^*$ transition form factor: Diamonds – result obtained with the physical current-quark mass value of 5.5 MeV; Circles – our chiral limit calculation; Solid line – the curve $(4\pi^2/3)$ $(-<\bar{q}\,q>/Q^4)$.

a.5. Charge Form Factors of Quark-Model Pions[1] (F. Coester and W. N. Polyzou*)

Experimental data on the pion charge form factor are well represented by Poincaré invariant constituent-quark phenomenology depending on two parameters, a confinement scale and an effective quark mass. Pion states are represented by eigenfunctions of mass and spin operators, and of the light-front momenta. An effective current density is generated by the dynamics from a null-plane impulse current density. A simple shape of the wave function depending only on the confinement scale is sufficient. The range of quark-masses and confinement scales consistent with both low and high Q^2 data depends on the shape of the wave function. Such minimal phenomenological models of confined quark dynamics with quark masses between 200 and 300 MeV can easily accommodate existing experimental values of pion form factors, as well as QCD based predictions for Q^2 in the range of several GeV^2. Sufficiently precise data for larger values of Q^2 will limit acceptable shapes of the wave functions and associated mass scales of the impulse currents.

*University of Iowa.

[1] F. Coester and W. N. Polyzou, Phys. Rev. C **71**, 028202 (2005).

a.6. Axial Transition Form Factors and Pion Decay of Baryon Resonances[1] (F. Coester, B. Juliá-Díaz,* and D. O. Riska*)

The pion decay constants of the lowest orbitally excited states of the nucleon and the Δ(1232) along with the corresponding axial transition form factors are calculated with Poincaré covariant constituent-quark models with instant, point and front forms of relativistic kinematics. The model wave functions are chosen such that the calculated electromagnetic and axial form factors of the nucleon represent the empirical values in all three forms of kinematics, when calculated with single-constituent currents. The closest description of the empirical values for the axial coupling of the nucleon and the *Δ(1232)-N* axial transition coupling obtains with front form kinematics. The pion decay widths calculated in instant and point form are significantly smaller than in front-form kinematics.

*University of Helsinki, Finland.

[1]B. Juliá-Díaz, D. O. Riska, and F. Coester, Phys. Rev. C **70,** 045204 (2004).

a.7. Quark-Hadron Duality and Parity Violating Asymmetry of Electroweak Reactions in the Δ Region (T.-S. H. Lee, K. Matsui,* and T. Sato*)

A dynamical model of electroweak pion production reactions in the *Δ(1232)* region, developed by Sato and Lee, was extended to include neutral current contributions in order to examine local Quark-Hadron Duality in neutrino-induced reactions and to investigate how the axial *N-Δ* form factor can better be determined from the parity violating asymmetry in $N(\vec{e}\,,e')$ reactions. We showed that recent *(e,e')* data on the structure functions F_1 and F_2, which exhibit Quark-Hadron Duality, are in good agreement with our predictions. For possible future experimental tests, we then predicted that the structure functions F_1, F_2, and F_3 for *(ν,e)* and *(ν,ν')* processes should also show a similar Quark-Hadron Duality. These results are shown in Fig. V-3. The spin dependent structure functions g_1 and g_2 in *(e,e')* were also calculated in our model. It was found that local Quark-Hadron Duality is not seen in the calculated g_1 and g_2, while our results for g_1 and some polarization observables associated with the exclusive $p(\vec{e}\,,e'\pi)$ and $\vec{p}\,(\vec{e}\,,e\pi)$ reactions are in good agreement with recent data. This is shown in Fig. V-4. In an investigation of the parity violating asymmetry A of $N(\vec{e}\,,e')$ reactions, it was found that the non-resonant contribution is small at the Δ peak and a measurement of A with an accuracy of 20% or better is needed to distinguish two previously determined axial *N-Δ* transition form factors. This is shown in Fig. V-5. The predicted asymmetry A is also compared with Parton Model predictions for future experimental investigations of Quark-Hadron Duality.

*Osaka University, Japan.

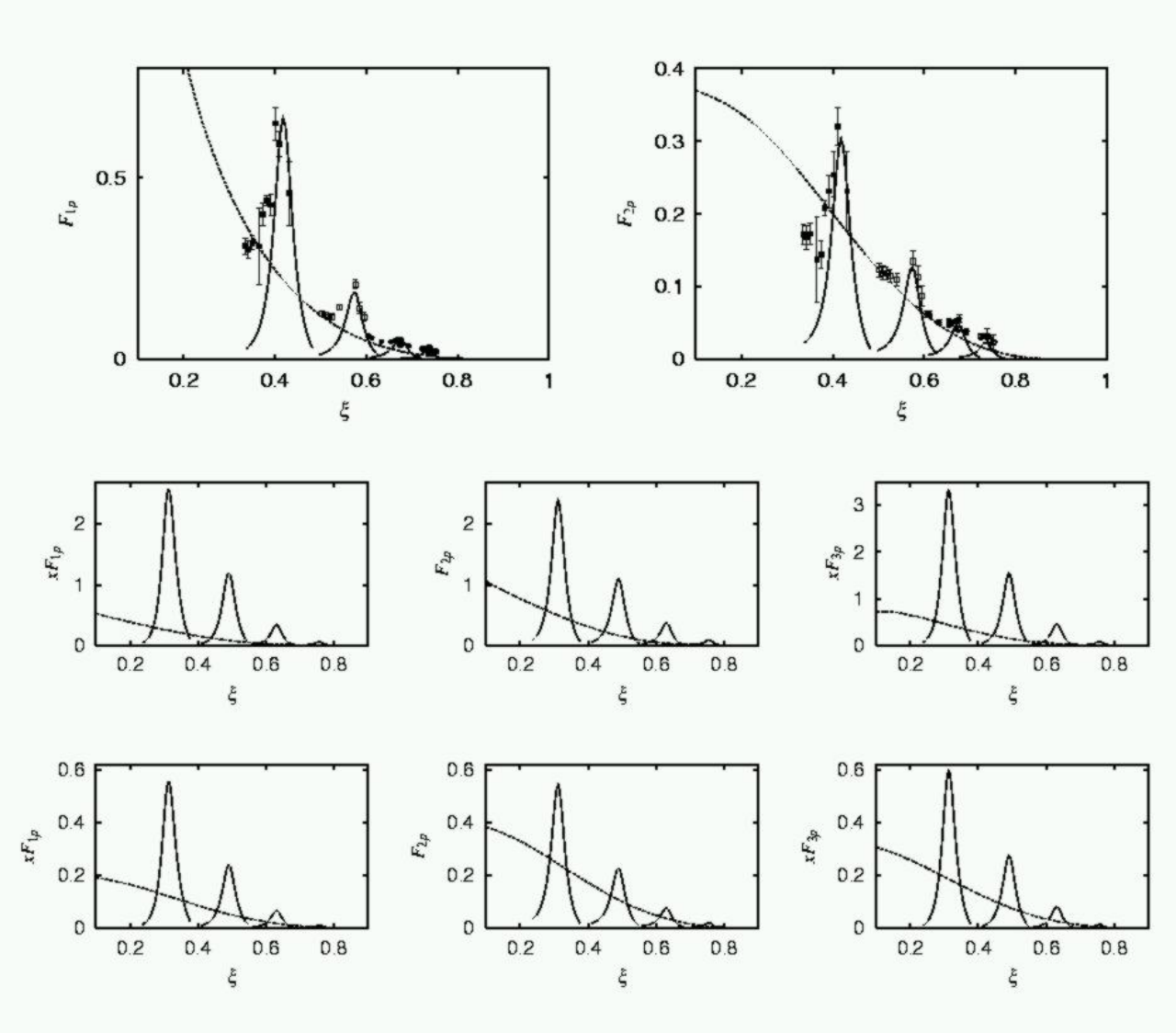

Fig. V-3. Structure functions F_1 (left) and F_2 (right) of p(e,e') (top), and F_1 (left), F_2 (center), and F_3 (right) for p(ν,e$^-$) (middle) and p(ν,ν') (bottom) processes. The dashed curves are calculated using the CETQ6 parton distribution functions at Q^2 = 10 (GeV/c)^2. The solid curves are the results at Q^2 = 0.7,1.5,2.3,3.5 (GeV/c)^2 (from left to right) calculated with the SL model.

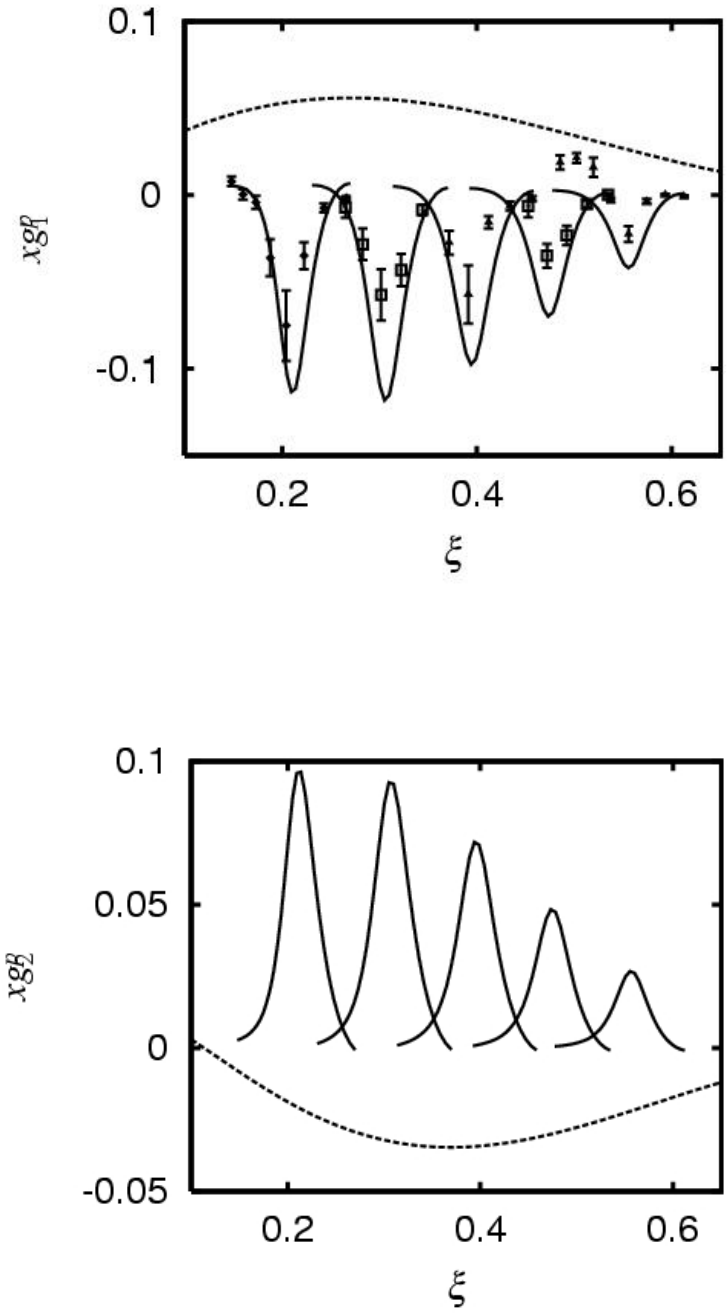

Fig. V-4. Spin dependent structure functions g_1 (top) and g_2 (bottom). The dashed curves are from the fits to deep inelastic scattering data. The solid curves are the results at Q^2 = 0.21, 0.35, 0.62, 0.92, 1.37 $(GeV/c)^2$ (from left to right) calculated with the SL model.

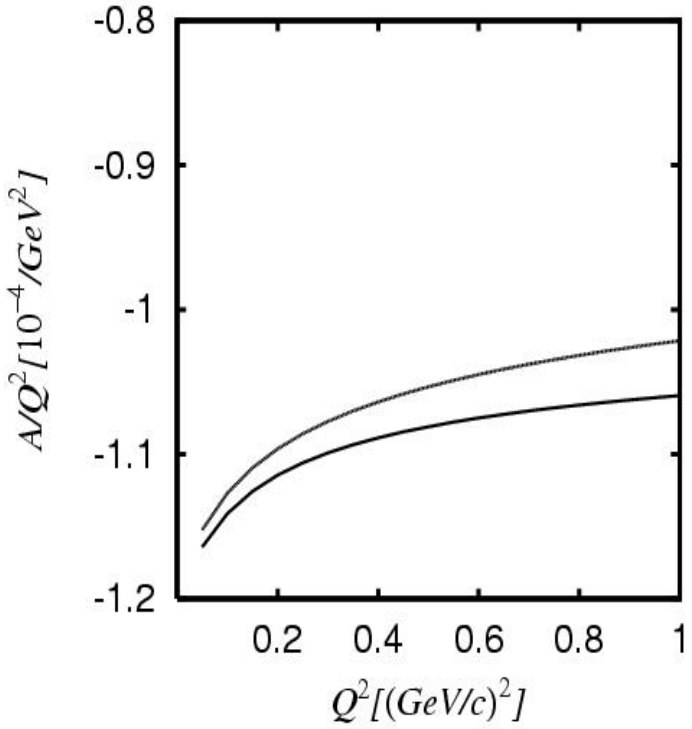

*Fig. V-5. The Q^2-dependence of the parity violating asymmetry (A/Q^2) of $\vec{p}$ (e,e') calculated with the SL model. The solid (dashed) curve is obtained using the axial N-Δ form factor G_N^A, Δ of the SL model [Kitagaki et al., Phys. Rev. D **42**, 1331 (1990)]. The results are for invariant mass W = 1.232 GeV and electron scattering angle θ = 110°.*

a.8. Dynamical Coupled-Channel Model of Electromagnetic Meson Production Reactions (T.-S. H. Lee, A. Matsuyama,* and T. Sato†)

We have developed a dynamical coupled-channel model for investigating the structure of the nucleon resonances *(N*)* using the very extensive data from Jefferson Laboratory. The model Hamiltonian includes interactions between γN, πN, ηN, ωN, and the three-body $\pi\pi N$ ($\pi\Delta$, ρN, σN) channels. Meson cloud effects on the *N** excitations are treated exactly, consistent with the $\pi\pi N$ unitarity condition. The non-resonant parts of the model Hamiltonian are derived from effective Lagrangians by using the unitary transformation method. The *N** parameters are identified with current hadron structure calculations. The resulting Faddeev-type coupled-channel scattering equations are solved by using a Spline-Function method such that the $\pi\pi N$ cut effects can be included exactly in calculating the meson production cross sections. This crucial numerical advance overcame the main difficulty of all of the previous work using the method of contour rotation. We are now applying the method to analyze the JLab data on $\gamma p \rightarrow \pi\pi N$. One sample result from our calculations at $W = 1.7$ GeV is shown in Fig. V-6. We see that the model can reproduce the main features of the data. We are in the process of exploring whether the remaining discrepancies with data can be interpreted as the contributions from 'missing' *N** resonances.

*Shizuoka University, Japan; †Osaka University, Japan.

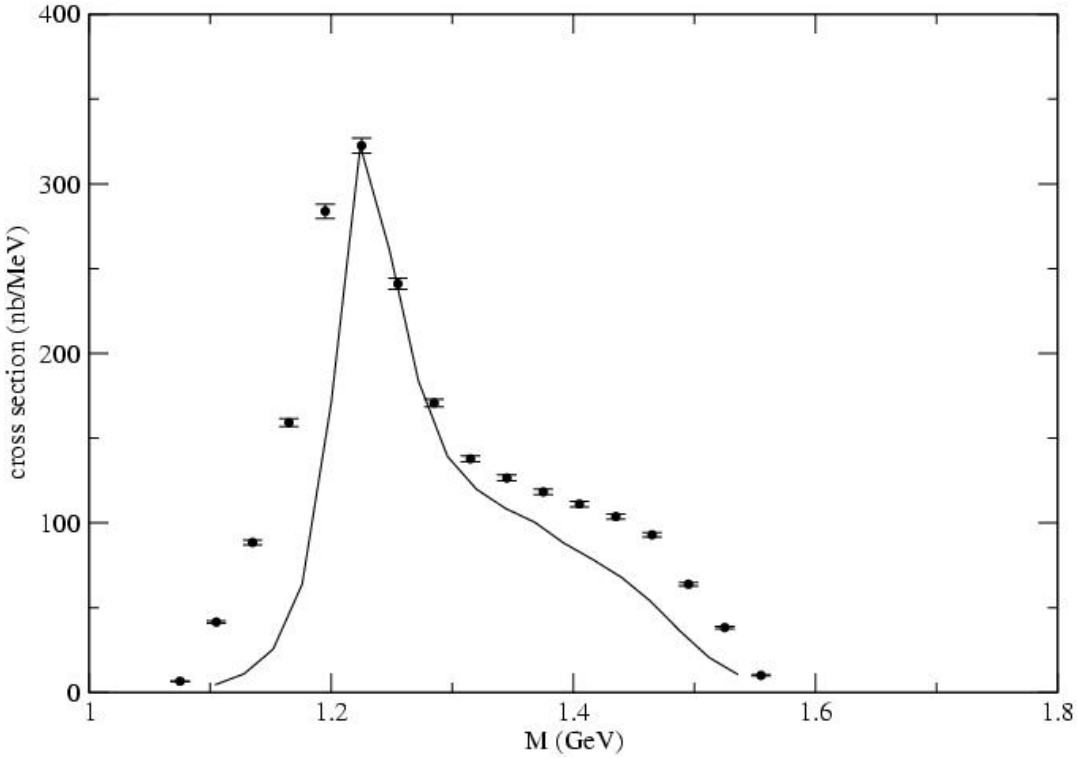

Fig. V-6. The calculated $\gamma p \rightarrow \pi^- \pi^+ p$ cross section as a function of the invariant mass of the final $\pi^+ p$ system (solid line) is compared with the JLab data at W = 1.7 GeV.

a.9. Study of N* Resonances with Kaon Photoproduction Reactions (T.-S. H. Lee, B. Julia-Diaz,*† B. Saghai,* and F. Tabakin†)

We are performing coupled-channel calculations in order to investigate N^* effects in kaon photoproduction reactions. The model consists of γN, πN, KY ($K\Lambda$ and $K\Sigma$) channels. The effects due to other channels, such as the $\pi\pi N$, are treated phenomenologically by using a subtraction method and empirical γN and πN amplitudes. On the other hand, the crucial final state interactions owing to $\pi N \rightarrow KY$ and $KY \rightarrow K'Y'$ are generated from a coupled-channel model, which is derived from an *SU(3)* effective Lagrangian and describes well the available $\pi N \rightarrow KY$ data. In Fig. V-7, we show a sample result from our calculations. It is seen that: the coupled-channel effect owing to the πN channel is important; and the N^* excitations play an important role in strangeness production reactions. We are now in the process of analyzing all $\gamma N \rightarrow K\Lambda, K\Sigma$ data from Jefferson Laboratory, aiming at testing the N^* parameters predicted by chiral constituent quark models.

*CEA/Saclay, France, †University of Pittsburgh.

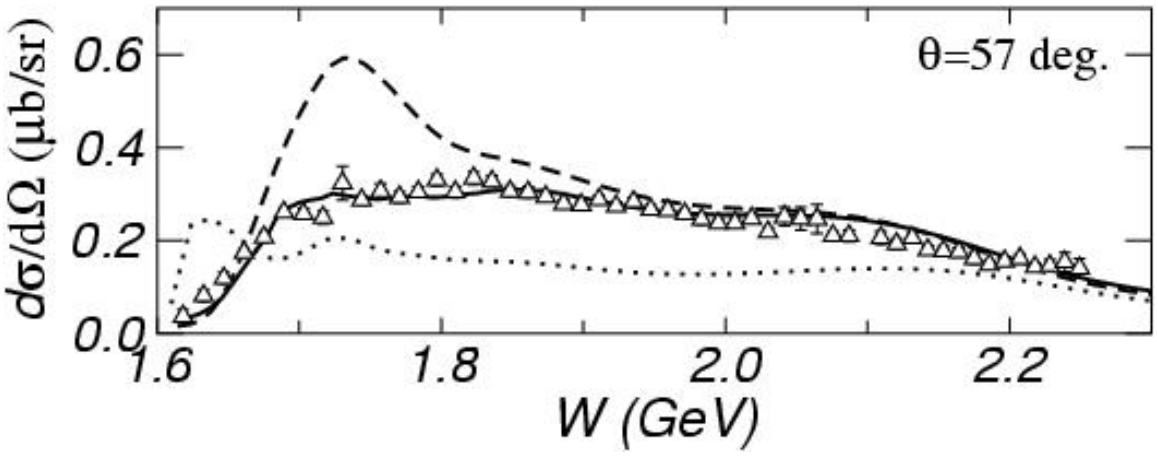

Fig. V-7. Total cross sections for $\gamma p \to K^+\Lambda$. The solid curve is our full coupled-channel calculation. The dashed curve is obtained when the coupling with the πN channel is turned off. The dotted curve is from keeping only the N effects.*

a.10. Medium Effects on the Electromagnetic ρ Meson Production on Nuclei

(T.-S. H. Lee, Y. Oh,* and R. Rapp†)

It is recognized that in-medium effects on vector meson propagation are crucial in understanding di-lepton production in relativistic heavy-ion collisions. In particular, the effects predicted by Rapp and Wambach have provided a quantitative explanation of the di-lepton production data without invoking the assumption that a quark-gluon plasma was created during the collision. On the other hand, the predicted in-medium effects must be verified in other reactions that do not have the complexities of relativistic heavy-ion collisions. We are conducting such an investigation by considering the photoproduction of ρ meson on nuclei. The ρ photoproduction amplitude is generated from the model of Oh and Lee, and the ρ propagation in finite nuclei is calculated from the model of Rapp and Wambach by applying the Eikonal formulation of Gottfried and Julius. We are in the process of developing a computation code for analyzing the recent JLab data obtained by Argonne's Medium Energy Group.

*University of Georgia; †Texas A&M University.

a.11. Pentaquark $\Theta^+(1540)$ Production in $\gamma N \to K\bar{K}N$ Reactions

(T.-S. H. Lee, K. Nakayama,* and Y. Oh*)

We investigate how the exotic pentaquark *Θ(1540)* baryon can be identified in the $\gamma N \to K\bar{K}N$ reactions, focusing on the influence of the background (non-*Θ* production) mechanisms. By imposing the *SU(3)* symmetry and using various quark model predictions, we are able to fix the coupling constants for evaluating the so-called Drell diagrams, the $K\bar{K}$ production through the intermediate vector meson and tensor meson photoproduction, and the mechanisms involving intermediate *Λ(1116), Λ(1405), Λ(1520), Σ(1193), Σ(1385),* and *Δ(1232)* states. The vector meson photoproduction part is calculated from a phenomenological model which describes well the experimental data at low energies. The charged tensor meson production is calculated from a one-pion-exchange model which describes well the total cross section data of $\gamma p \to a_2^+(1320)\, n$. We point out that the neutral tensor meson production cannot be due to π^0-exchange [as done by Dzierba *et al., Phys. Rev. D* ***69****, 051901 (2004)*] because of *C*-parity. Neutral tensor meson production is estimated by considering vector meson exchange and found to be too weak to generate any peak at the position near *Θ(1540)*. For *Θ(1540)* production, we assume that it is an isoscalar and hence can only be produced in $\gamma n \to K^+K^-n$ and $\gamma p \to K^0\bar{K}^0 p$ reactions, not in $\gamma p \to K^+K^-p$ and

$\gamma n \rightarrow K^0 \bar{K}^0 n$. The total cross section data for $\gamma p \rightarrow K^+ K^- p$ is thus used to fix the form factors which regularize the background amplitudes so that the signal of $\Theta(1540)$ in $\gamma n \rightarrow K^+ K^- n$ and $\gamma p \rightarrow K^0 \bar{K}^0 p$ cross sections can be predicted. We find that the predicted K^+K^- and K^+n invariant mass distributions in the $\gamma n \rightarrow K^+ K^- n$ reaction can qualitatively reproduce the shapes of the JLab data. However, the predicted $\Theta(1540)$ peak cannot be unambiguously identified in the data. This is shown in Fig. V-8. Our results suggest strongly that high statistics experiments are needed to resolve the problem.

*University of Georgia.

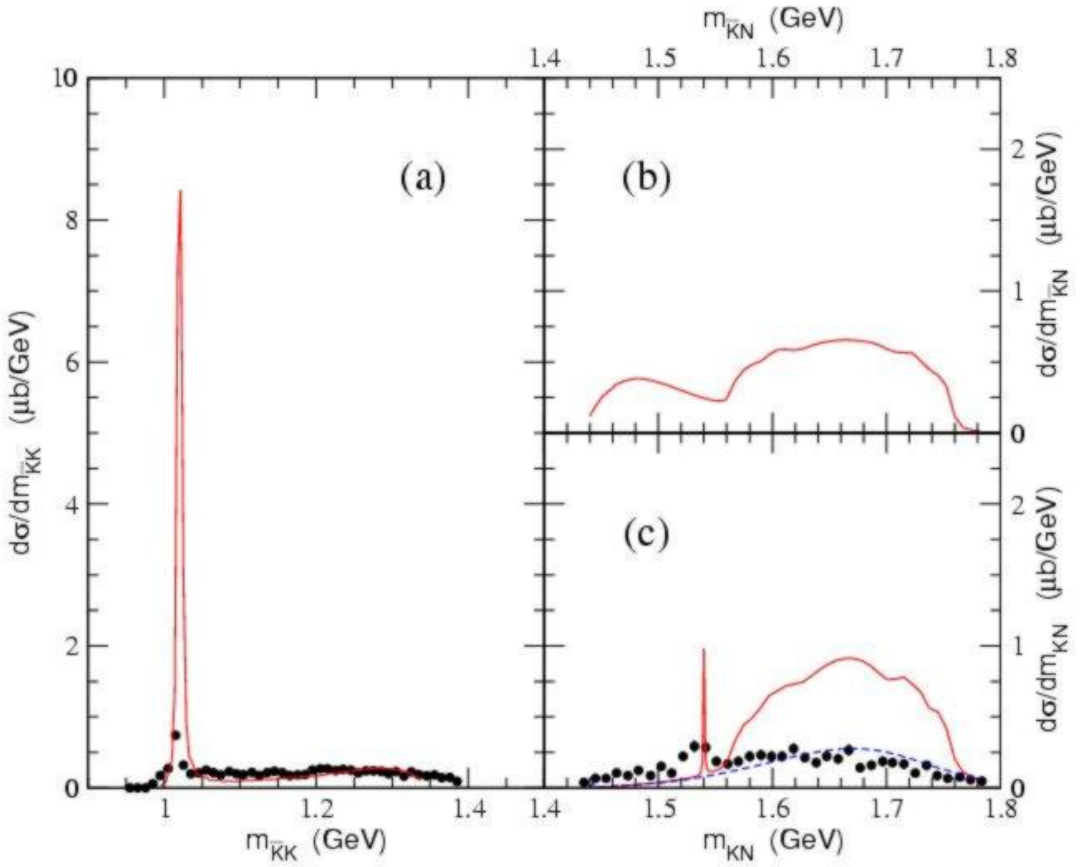

Fig. V-8. (a) $K\bar{K}$, (b) $\bar{K}N$, and (c) KN invariant mass distributions for $\gamma n \rightarrow K^+K^-n$ at E_γ = 2.3 GeV. The experimental data are from JLab. The dashed line in (c) is obtained without the φ meson background and the Θ contributions. Here we assume that the Θ(1540) has even parity.

B. NUCLEAR FORCES AND NUCLEAR SYSTEMS

The goal of this program is to achieve a description of nuclear systems ranging in size from deuterium and tritium to nuclear matter and neutron stars using a single parametrization of the nuclear forces. Aspects of our program include both the construction of two- and three-nucleon potentials and the development of many-body techniques for computing nuclear structure and reactions with these interactions. Detailed quantitative, computationally-intensive studies are essential parts of this program.

Quantum Monte Carlo (QMC) calculations of light ($A \leq 12$) nuclei with realistic interactions have been the main focus of our recent efforts. Our nonrelativistic Hamiltonian contains the accurate Argonne *v18* two-nucleon (*NN*) potential, which includes charge-independence breaking terms, and either the Urbana IX three-nucleon (*NNN*) potential, or one of several Illinois *NNN* models. The QMC calculations include both variational (VMC) and Green function (GFMC) methods. We begin with the construction of variational trial functions based on sums of single-particle determinants with the correct total quantum numbers, and then act on them with products of two- and three-body correlation operators. Energy expectation values are evaluated with Metropolis Monte Carlo integration and parameters in the trial functions are varied to minimize the energy. These optimized variational wave functions can then be used to study other nuclear properties. They also serve as a starting point for the GFMC calculations, which systematically remove higher excited-state components from the trial wave functions by propagation in imaginary time.

We are currently studying all $A \leq 10$ nuclei, including more than 100 ground or excited states, as well as ^{12}C. These are the first calculations to treat $A \geq 6$ nuclei directly with realistic *NN* and *NNN* interactions. In GFMC calculations, with our best Hamiltonian, we can reproduce most of the experimental ground- and excited-state energies to within *0.6 MeV*.

This year we reported a study of higher excited states in $A = 6$-8 nuclei, based on the discovery that GFMC propagation, when started with orthogonalized VMC wave functions for multiple states of the same spin and parity, preserves the orthogonality to a very good approximation. This has enabled the calculation of many more states in the last few years, and these studies are now being extended to $A \geq 9$ nuclei.

Many excited states in the light nuclei are not particle stable and should be treated as scattering states, though our efforts prior to this year treated all of them as bound. A major effort began this year to extend our GFMC program to nucleon-nucleus scattering, and substantial progress was made on ^5He, or n-α scattering. The results are promising, indicating an ability to calculate *ab-initio* the low-energy scattering cross section, and extract resonance energies and widths. A major long term goal of this effort is to use GFMC wave functions to predict reaction cross sections for astrophysics as part of the Theory Group's nuclear astrophysics effort.

We also began a systematic survey of cluster form factors and spectroscopic factors in the light *p*-shell nuclei using VMC wave functions. The correlations in these wave functions can provide significant quenching of spectroscopic factors compared to traditional shell-model calculations. Specific applications were made for two *(d,p)* experiments performed at ATLAS using rare-

isotope beams in inverse kinematics. The calculated cluster form factors were used as input to the distorted-wave Born approximation (DWBA) program PTOLEMY, developed here many years ago, to provide the theoretical analysis of the experiments.

b.1. Quantum Monte Carlo Calculations of Light Nuclei Energies

(S. C. Pieper, R. B. Wiringa, K. M. Nollett, and J. Carlson*)

We have been studying the ground states and excitation spectra of light nuclei as A-body problems with realistic nucleon-nucleon (NN) and three-nucleon (NNN) interactions using advanced quantum Monte Carlo (QMC) many-body methods. Our preferred Hamiltonian contains the Argonne v_{18} NN potential (AV18), which gives an excellent fit to elastic NN scattering data and deuteron properties, and the Illinois-2 NNN potential (IL2), which we have fit to binding energies of $A \leq 8$ nuclei. The QMC methods include both variational Monte Carlo (VMC), which gives an initial approximate solution to the many-body Schrodinger equation, and Green function Monte Carlo (GFMC), which systematically improves on the VMC starting solution. The GFMC method produces absolute binding energies that are accurate at the 1-2% level.

The VMC calculations begin with the construction of an antisymmetric Jastrow trial wave function that includes single-particle orbits coupled to the desired JM values of the state of interest as well as pair and triplet correlations. A symmetrized product of two- and three-body spin, isospin, and tensor correlation operators (induced by the NN and NNN potentials) is applied to the Jastrow product to produce the full trial function. The wave function is diagonalized in the small basis of different spatial symmetry components to project out multiple states with the same quantum numbers.

In GFMC calculations an imaginary-time propagator, $exp[-(H-E_0)\tau]$, where H is the Hamiltonian, E_0 is an estimate of the eigenvalue, and τ is the imaginary time, is applied to the VMC trial function. The excited-state components of the trial function are damped out for large τ, leaving the exact lowest eigenfunction with the quantum numbers of the input VMC trial function. The expectation value of H is computed for a sequence of increasing values of τ to determine the convergence.

Two years ago we found that GFMC can be used to compute higher excited states with the same quantum numbers as lower states if the propagation is started with a trial function that is orthogonal to the starting wave functions for the lower states. This past year we systematically computed all the p-shell states in the $A = 6,7,8$ nuclei, doubling the number of states we had been able to study previously. The excited state spectrum is shown in Fig. V-9. With our best Hamiltonian, AV18+IL2, we reproduce 36 experimental energies with an rms deviation of 0.60 MeV.[1] This work is being extended to additional excited states in the $A = 9,10$ nuclei.

Recently we began studying p-shell nuclei with incomplete s-shell cores, such as ^4H, negative-parity excited states in ^4He, ^5H, ^7H, etc., with the VMC method. In the $A = 4$ cases, we get reasonable qualitative agreement with R-matrix analyses of experimental data, although ultimately these systems should be studied as $(A-1) + N$ scattering states, as discussed below for ^5He. However for the heavier hydrogen isotopes, which are not well known but are the subject of experimental searches, we may have to settle for pseudo-bound-state calculations for some time. GFMC results have also been obtained for the ground states of $^{4,5}H$.

We are also working on unnatural-parity states caused by the excitation of one p-shell nucleon to the sd-shell. These states can appear fairly low in the excitation spectrum of $A \geq 7$ nuclei, and particle-stable states occur in ^{10}Be and ^{10}B. First calculations of such states a few years ago found them to be several MeV higher than observed experimentally. Recently we revisited the ^9Be positive-parity states and obtained much better results. We also studied ^7He positive-parity states for the first time in support of an ATLAS experiment, discussed below in connection with spectroscopic factors. We plan to revisit the $A = 10$ states in the coming year.

*Los Alamos National Laboratory.

[1] S. C. Pieper, R. B. Wiringa, and J. Carlson, Phys. Rev. C **70**, 054325 (2004).

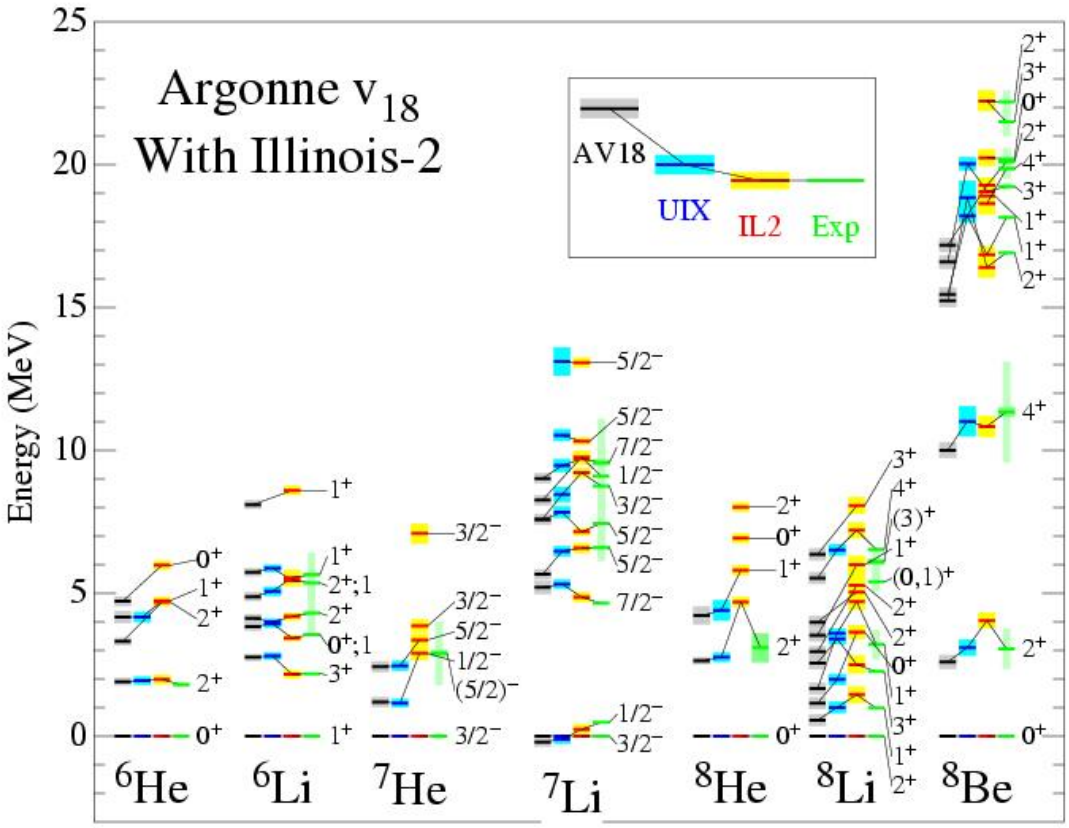

Fig. V-9. GFMC excitation energies computed for the Hamiltonians AV18, AV18 + UIX, and AV18 + IL2, compared with experimental values. The shaded bands show the Monte Carlo statistical (or experimental) errors. The narrow shaded bars on the experimental values show the experimental widths.

b.2. Scattering Methods for Quantum Monte Carlo Calculations (K. M. Nollett, S. C. Pieper, R. B. Wiringa, and J. Carlson*)

Our calculations of properties of light nuclei have concentrated on computing energies, particularly since the development of the methods has until recently required that unbound states be treated as bound states. We have therefore been restricted to bound or narrow states, and unable to compute the widths of resonances. A smaller amount of effort has gone into computing transition probabilities and radiative-capture cross sections using VMC wave functions, along with calculations of a few static nuclear properties like RMS radii.

It is desirable to expand the range of the QMC methods to include unbound states treated as such and the computation of phase shifts and reaction cross sections. This will greatly expand the number of observables against which the potentials can be tested. It will also open the door to accurate quantitative predictions of reaction cross sections for astrophysics, at least in the light systems important for solar neutrinos, big-bang nucleosynthesis, and seeding the *r*-process in neutron-rich freezeout.

We are developing methods to compute unbound states, using an *R*-matrix-like boundary condition to specify the state being computed. As a first application, we have computed low-energy phase shifts in the first three partial waves in ^{4}*He-n* scattering. In VMC, the boundary condition is set as a condition on the correlation between the ^{4}*He* nucleus and the last neutron. In GFMC, the boundary condition is enforced through a method of images that enforces a specified logarithmic derivative in the wave function at a specified surface (a fixed ^{4}*He-n* separation, usually 7 or 8 fm in our calculations).

Preliminary results are in good agreement with *R*-matrix fits to the laboratory data. These are shown in Fig. V-10 b for the Argonne-v_{18} + Illinois-2 potential. This potential reproduces the experimental energies for the given boundary conditions to within *0.2 MeV* for ^5He states with $J = 3/2$ and *0.5 MeV* for states with $J = 1/2$. This compares favorably with its performance for the 17 narrow or bound states to which it was fitted.

This work opens the door to several additional calculations in light nuclei, particularly neutron resonances, states in ^4H, and the $^7Be(p,\gamma)^8B$ radiative capture reaction.

*Los Alamos National Laboratory.

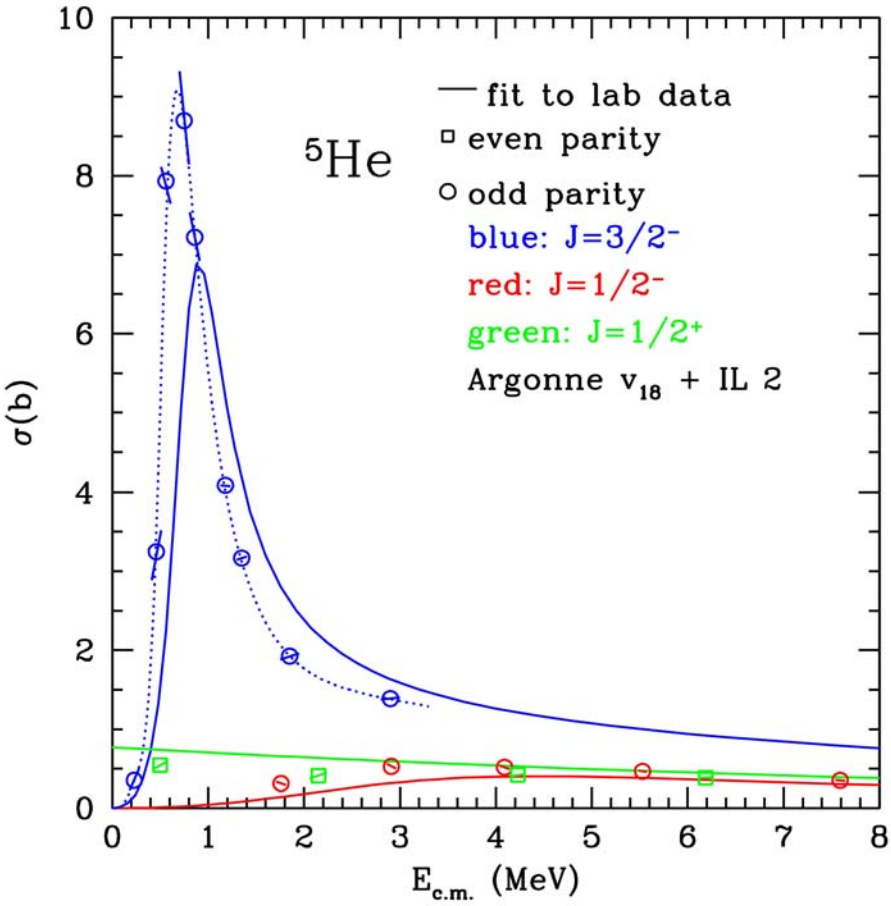

Fig. V-10. Cross sections for ^{4}He-neutron scattering, broken down by partial wave. Solid curves are an R-matrix fit to the measured cross sections. Points with Monte Carlo error bars are results of GFMC calculations. The blue dotted curve connecting the $J^\pi = 3/2^-$ results is a guide to the eye.

b.3. Spectroscopic Factors and Cluster Form Factors of Light Nuclei (R. B. Wiringa, S. C. Pieper, D. Kurath, and D. J. Millener*)

The cluster form factor is defined as the overlap between *A*-body and *(A-1)*-body nuclear states, either in configuration or momentum space, $\langle (A\text{-}1)_J | a_j(r,p) | A_J' \rangle$, where a_j is a nucleon annihilation operator. It is a very useful quantity in analyzing pickup reactions such as *(p,d)*, where A_J' is a ground state, or stripping reactions such as *(d,p)*, where $(A\text{-}1)_J$ is a ground state, or nucleon-knockout reactions such as *(e,e'p)*. The cluster form factor can be folded into a DWBA calculation to help extract experimental

information. The spectroscopic factor S is just the normalization of this wave function overlap, and provides a simple characterization of nuclear structure aspects of such reactions.

We have been calculating the cluster form factors and spectroscopic factors for all $A \leq 10$ nuclei using VMC wave functions from the AV18+UIX Hamiltonian. The spectroscopic factors are being compared to predictions from the Cohen-Kurath (CK) shell model. The CK spectroscopic factors for transitions between stable nuclei were first published in 1967, but many additional transitions are now experimentally accessible with the advent of rare-isotope beams at Argonne, MSU, and other facilities.

The main difference between the CK and VMC spectroscopic factors is that the latter can show significant reductions due to the correlations in the VMC wave functions. An example is the $^{7}Li(e,e'p)^{6}He(J)$ reaction where $J = 0,2$ for the ground state or first excited state of the residual ^{6}He nucleus. The CK values for these two states are 0.59 and 0.40, while the VMC calculation gives 0.36 and 0.25, respectively, or just 2/3 the strength. This kind of reduction in strength is consistent with electron-scattering experiments. However, the VMC spectroscopic factors are not always significantly reduced compared to CK, indicating considerable dependence on details of the nuclear structure.

As part of this work, the effect of translational invariance on spectroscopic factors was studied. We find that for light p-shell nuclei described by realistic wave functions, the effect of translational invariance is much smaller than the standard shell-model correction of $A/(A-1)$. We are continuing to study this.

Two specific applications were made this year in conjunction with experiments carried out at ATLAS with rare-isotope beams. These were studies of the experimental spectrum of ^{9}Li using the $^{8}Li(d,p)^{9}Li$ reaction, and a search for excited states in ^{7}He using the $^{6}He(d,p)^{7}He$ reaction, both in inverse kinematics. We computed excited state spectra for ^{9}Li and ^{7}He, including positive-parity states in the latter case. We then evaluated the cluster form factors for transitions to the different states and fed them into the DWBA program PTOLEMY to compare theoretical predictions with experimental differential cross sections. For ^{9}Li the DWBA results are generally in good agreement with experiment, both for the magnitude and shape of the angular distributions.[1] For ^{7}He the ground-state distribution is well described, but a large, broad, peak around 2.5 MeV excitation energy can only be partially accounted for.

---

*Brookhaven National Laboratory.

[1] A. H. Wuosmaa *et al.*, Phys. Rev. Lett. **94**, 082502 (2005).

C. NUCLEAR ASTROPHYSICS

The objective of this research program is to investigate nuclear processes that take place in stars, in the big bang, and in interstellar and intergalactic space. Nuclear phenomena are ubiquitous in the universe. The stars shine by nuclear energy, and the chemical compositions observed in the solar system and elsewhere are the results of nuclear processes that occurred in the big bang and inside the several generations of stars that have formed since then. Many astrophysical phenomena may only be understood by a combination of nuclear physics with methods more familiar to astrophysicists.

A particularly important problem is to determine rates for the nuclear reactions that occur in astrophysical environments. There are many applications (for example, the rapid neutron capture process) where large contributions from theoretical nuclear physics – particularly masses and cross sections - will always be necessary as input, and we maintain research interests in these areas. We have applied advances in the theoretical descriptions of light nuclei to compute cross sections important for big-bang nucleosynthesis, the solar neutrino flux, and seeding of the *r*-process. This work continues in close connection with our other work on light nuclei, and the main goals at present are to improve the wave functions and computational methods as described in section **b.2**. In the last year, we have participated in work to improve the computational methods used to compute weak-interaction rates important for the collapse and subsequent supernova explosions of massive stars.

Understanding nucleosynthesis and energy generation in a particular astrophysical environment requires calculations of nuclear reaction networks. Even for cases in which the detailed astrophysical phenomena can only be understood from difficult calculations coupling a reaction network and hydrodynamics, simpler network calculations can identify the crucial reactions and other nuclear properties to be determined by more detailed theoretical and experimental work. Ongoing work in this area involves big-bang nucleosynthesis, nuclear burning in low-mass stars, and photon-nucleus reactions in high-energy cosmic rays.

A major goal of nucleosynthesis studies is to determine the specific physical conditions that gave rise to abundance patterns seen in nature: what mix of different kinds of stellar environments gave rise to observed chemical compositions? Large amounts of important new data on abundance patterns are now being collected, with important evidence arising from low-metallicity stars in our own galaxy, absorption-line systems backlit by distant quasars, and primitive inclusions and pre-solar grains embedded in meteorites. These data contain important clues about the nucleosynthetic history of the universe, both locally and globally, and the effort to disentangle the clues into information on stellar sources and galactic chemical evolution is necessarily coupled to our work on nucleosynthesis.

In addition, studies are underway of electroweak reaction rates relevant to astrophysical processes in dense nuclear matter. These are a part of our attempt to predict observable features of quark matter in compact astrophysical objects.

c.1. Moments Methods for Response Functions with Momentum Transfer Dependence

(K. M. Nollett, W. Haxton,* and K. Zurek*)

Models of the pre-supernova evolution of massive stars are very sensitive to the neutrino transport properties of the stellar core, which in turn have large contributions from inelastic neutrino scattering on nuclei in the mass range near iron. Much of the scattering response of these nuclei is dominated by the Gamow-Teller resonance. In a shell-model approach, this contribution to the cross section can be separated into an energy-dependent factor and a separate response function that is independent of momentum transfer q. The response function is found by the Lanczos algorithm, an iterative procedure that casts the Hamiltonian into a tridiagonal form given a suitably-chosen initial basis vector. To find a response function, one applies the operator of interest (in this case, the Gamow-Teller operator) to the initial state, and uses the resulting state as the starting point in a Lanczos tridiagonalization. The eigenvectors of the tridiagonal matrix are then easily related to the response function of the operator.

To determine Gamow-Teller rates averaged over a neutrino energy distribution, one need only apply this procedure once. However, there may be significant contributions from forbidden transitions, introducing more complicated q dependence into the operator, so that the response function has to be recomputed completely for each q. In the usual shell model approach for nuclei of mass comparable to iron, this is computationally prohibitive. Hence, groups who found Gamow-Teller strengths from the Lanczos procedure have switched to the random-phase approximation in order to incorporate forbidden transitions in their calculations.

We have taken a different approach and sought ways of breaking up the Lanczos algorithm into first a computationally-expensive setup phase that is performed only once and then a much smaller set of steps that take information computed in the first phase and produce the response function at a given value of q. With this in mind, we have produced four new variations on the Lanczos algorithm, and tested them by application to the problem of inelastic electron scattering on ^{28}Si – a problem that contains many of the same kinds of operators as the calculation of weak responses. Each algorithm has distinct strengths and weaknesses that will determine in what cases it is applicable, and all the algorithms are very similar in how they scale with the number of values of q at which the response is to be computed and the size of the shell-model basis. Each method also may be computed to reproduce the true strength function to some specified degree of precision, as shown in Figs. V-11 and V-12.

All of the methods are faster than the traditional Lanczos algorithm by a factor of the ratio of the dimension of the Hamiltonian to the number of values of q at which the response is to be computed. This will always be a large number (several orders of magnitude) for the astrophysical applications that we have in mind.

*University of Washington.

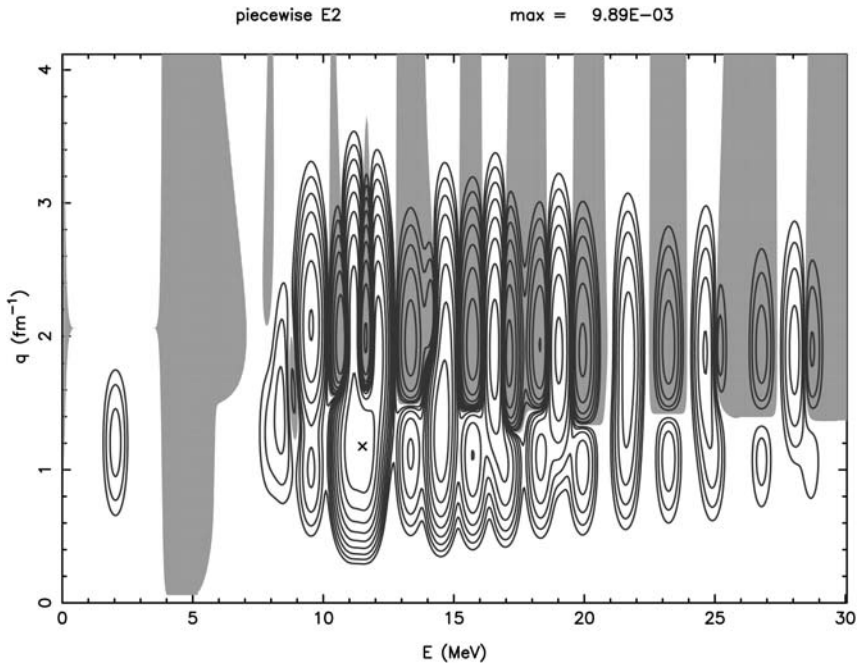

Fig. V-11. Contour plot of the E2 response function of ^{28}Si, computed by one of our new algorithms, the "piecewise Lanczos algorithm." The result has been computed to reproduce 60 moments of the function at a given energy exactly, then smoothed along the E direction by convolution with a Gaussian of full width 0.25 MeV. Shaded areas are regions of negative response, and contours are spaced logarithmically by factors of two.

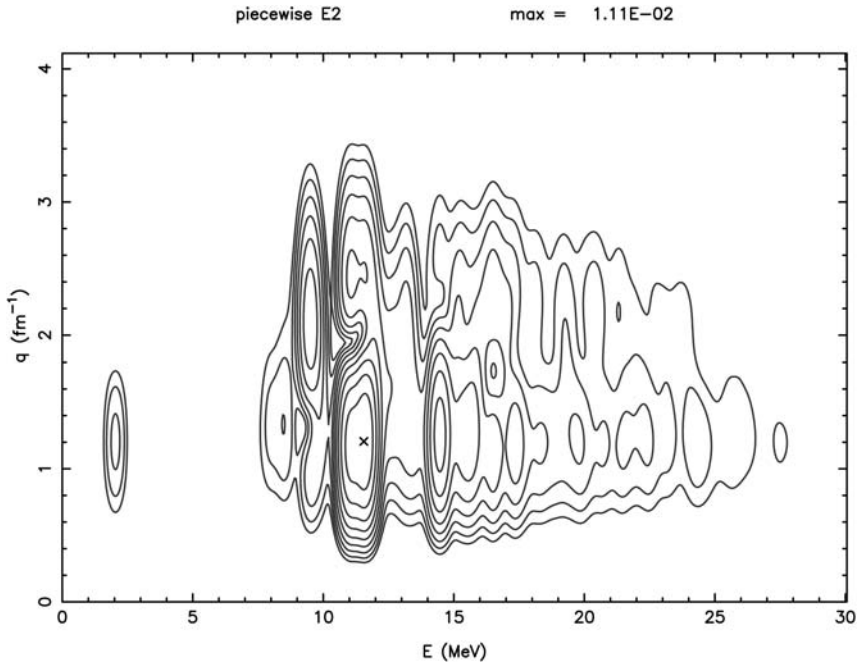

Fig. V-12. Same as Fig. V-11, but with 480 moments exact. Note the disappearance of (gray) regions of negative strength in the improved approximation to the positive-definite true response.

c.2. Short-Lived Nuclei in the Early Solar System and AGB Stars (K. M. Nollett, G. J. Wasserburg*, M. Busso†, and R. Gallino‡)

Sun-like stars, with masses below $3M_{\odot}$, are important sources of nuclei. They produced about half the nuclei heavier than iron in the solar system, a large fraction of the carbon, and possibly most of the nitrogen. In addition, the most numerous type of pre-solar grains recovered from meteorites, the "mainstream" grains, almost certainly formed in the ejecta from such stars.

Composition data from the meteorite grains and from astronomical observations suggest that there are mixing processes inside low-mass stars during the final red giant branch and asymptotic giant branch (AGB) stages, in addition to those processes present in standard one-dimensional stellar evolution models. We previously computed the effects of slow mixing of composition between the convective envelope of a $1.5M_{\odot}$ star and the hotter layers below, during the final few million years of the star's existence on the AGB. This process is referred to as "extra mixing" or "cool bottom processing" (CBP). The calculations showed that without severely disrupting the star's energy budget, composition patterns in the oxygen isotopes found in pre-solar oxide grains may be explained. If mixing is sufficiently deep, the abundances of the short-lived ^{26}Al incorporated into oxide grains may be explained. The characteristic results of this extra mixing now define what are called the "Group 2" oxide grains. New calculations that we have carried out for stars of $2M_{\odot}$ and $3M_{\odot}$ and a range of metallicities, indicate that the qualitative results are almost independent of stellar parameters.

Since the radioactive ^{26}Al may be produced by CBP, there are also important consequences for the sources of the several radionuclides known to have been present in meteorites that formed when the solar system first condensed. There has long been a puzzle as to how much of the early solar system inventory of radionuclides came from various sources. Possible sources for radionuclides include input from a nearby supernova or AGB star just before the solar system condensed, production from ions accelerated by the magnetic field of the sun during its formation, or simply from accumulated nucleosynthesis by many generations of stars. It is desirable to find a consistent picture involving one or more of these sources that accounts for the origins of the radionuclides, particularly those with lifetimes of 1-100 Myr. AGB-star models for the origins of radionuclides were previously constrained partly by their ^{26}Al production. However, the possibility of substantial ^{26}Al from CBP removes this constraint on the model. At the same time, the number of measured early-solar-system radioactivities has expanded, and it appears that a more diverse range of sources is needed than previously thought. In particular, ^{10}Be can only be made outside stars, and ^{53}Mn cannot come from AGB stars. Divergent results for abundances of ^{129}I, ^{182}Hf, and ^{247}Cm require at least three distinct sources of *r*-process nuclei that made their last contributions to the protosolar nebula at different times prior to formation of solids in the solar system.

*California Institute of Technology, †University of Perugia, Italy, ‡University of Torino, Italy.

D. NUCLEAR STRUCTURE AND HEAVY-ION REACTIONS

This research focuses on nuclear structure in unusual regimes: nuclei far from stability, and superdeformed nuclei at high spin. We also study heavy-ion reactions near the Coulomb barrier. Much of this work is closely tied to experiments performed at ATLAS and at radioactive beam facilities.

Our studies of heavy-ion reactions include coupled-channels calculations of fusion reactions, elastic and inelastic scattering. The calculated fusion cross sections are usually quite sensitive to the structure and the radii of the reacting nuclei, and it is often possible to reproduce the measurements quite well. However, the calculations can be challenging for very heavy systems because the couplings are strong and the calculations become sensitive to higher-lying states. Another difficulty occurs at energies far below the Coulomb barrier, where the measured cross sections start to fall off steeply compared to calculations.

The hindrance of heavy-ion fusion at low energy is a general phenomenon which has now been observed in many systems, ranging from medium-heavy to heavy systems. The hindrance can be seen clearly by plotting the S factor for fusion. The S factor develops a maximum at low energy, and the energy where that occurs is a good way to characterize the phenomenon. The fusion hindrance is expected to be an entrance channel effect because it occurs at a rather high value of the excitation energy of the compound nucleus, but it has so far not been possible to explain it by conventional coupled-channels calculations.

As part of our continued interest in extracting the rate of radiative capture reactions from experiments, we have focused on proton capture on ^{7}Be, which is relevant to the production of ^{8}B in the sun. We have completed a study of the constraints one can obtain on the capture rate from charge symmetry and from the experimental information about the $^{7}Li(n,\gamma)^{8}Li$ reaction. The result of the study is not unreasonable in comparison to most measurements but it is smaller than the most accurate direct capture measurements.

Many measurements of the $^{7}Be + p$ capture rate have been performed in recent years, using both direct and indirect methods. One indirect method is to measure the Coulomb dissociation of ^{8}B on a high-Z target and from the data analysis to extract the $^{7}Be + p$ capture rate. The results obtained are often smaller than the results of direct capture measurements, and it is of interest to understand what causes the discrepancy. We have therefore tested the validity of the first-order approximation that is commonly used in the analysis of Coulomb dissociation experiments by comparing it to more complete dynamical calculations, which include the excitation of ^{8}B to all orders in the Coulomb and nuclear fields from the target. We find that it is necessary to go beyond the conventional first-order analysis if accuracies of 10% or better are required in the extracted capture rate.

We are continuing the development of a program for calculating many-body variational wave functions. This approach puts pairing and particle-hole interactions on an equal footing. These wave functions strictly conserve particle-number and parity. Particle number and parity are projected before variation. In studies of nuclides near the $N = Z$ line, we also project states of good Q, the number parity of $T = 0$ pairs, before variation.

Our treatment of *n-p* pairing explains many features of nuclear structure for nuclei having almost equal numbers of protons and neutrons. These wave functions explain the Wigner energy anomaly in a simple way. This treatment also explains why the $T = 0$ 1^+ state is highly excited in $N = Z$ even-even nuclei and close to ground in odd-odd $N = Z$ nuclides.

We have developed a code for configuration mixing of the wave functions used to describe *n-p* pairing. We have applied these wave functions to explore *n-p* pair transfer probabilities in $N = Z$ nuclides. We find that this quantity is very sensitive to $T = 0$ and $T = 1$ correlations in the many-body wave function. Experimental measurements of the pair transfer probability, now under way, will establish the magnitude of $T = 0$ pairing interaction correlations in nuclei near the $N = Z$ line.

The low-lying states of odd mass nuclei provide a good test of the parametrizations of single particle potentials. Study of the spectroscopy of the heavy elements is particularly valuable, as it gives insights into the structure of super-heavy elements. In a collaborative effort with the experimental spectroscopy group at Argonne, we have analyzed low-lying neutron and proton single particle states in the mass 250 region. We have studied neutron single-particle states in ^{247}Cm and proton single particle states in ^{249}Bk, and determined single-particle potentials that are consistent with these analyses.

We also worked toward the development of a universal model for the systematic description of heavy nuclei by configuration mixing of symmetry-restored self-consistent mean-field states using modern effective-energy functionals. The tool developed was employed in large-scale calculations of nuclear properties; *e.g.*, the interpretation and prediction of properties of exotic nuclei.

d.1. Coupled-Channels Calculations of Heavy-Ion Fusion Reactions (H. Esbensen and C. L. Jiang)

We have continued our analysis of heavy-ion fusion cross sections using the coupled-channels technique. This approach works fairly well at energies in the vicinity of the Coulomb barrier and it is often possible to reproduce measurements by including in the calculations the couplings to the low-lying 2^+ and 3^- states, and the mutual and two-phonon excitations of these states. It is also necessary to include one- and two-nucleon transfer channels when the isospin asymmetry of projectile and target are very different.

There are limitations to the coupled-channels method. One example is heavy-ion fusion at energies far below the Coulomb barrier, where the measured cross sections are hindered compared to coupled-channels calculations. A very good example is the fusion of $^{64}Ni + ^{64}Ni$ which was measured at ATLAS.[1] It is possible to fit the data above 0.1 mb but the data below 0.1 mb fall off much steeper with decreasing energy than do the calculations. The hindrance of fusion at low energy is a general phenomenon, which has now been established for many heavy-ion systems.[2]

Coupled-channels calculations are also challenging for very heavy systems because the couplings are strong and it becomes necessary to include higher multi-phonon excitations in order to make the calculations converge. An example where this might happen is the fusion of $^{64}Ni + ^{100}Mo$ which was recently measured at ATLAS.[3] The quadrupole mode of ^{100}Mo is very soft and it is almost vibrational, as discussed in section ***d.2***. The calculations that were presented in Ref. 3 included up to three-phonon excitations of the soft quadrupole mode, in addition to the mutual and two-phonon excitations of other low-lying surface modes. We have improved these calculations by including up to six-phonon excitations of the soft quadrupole mode. The surprising result is that the calculated fusion cross section does not change much.

This is illustrated in the top part of Fig. V-13, where the six-phonon calculation (PH6) essentially falls on top of the three-phonon (PH3) calculation.

The effect of couplings to higher multi-phonon states can be seen in the barrier distribution, which is shown in the bottom part of Fig. V-13. The blue dashed curve is the barrier distribution for the three-phonon calculation (PH3) and the red solid curve is the distribution for the six-phonon calculation (PH6). They are very broad, almost 20 MeV, and some of the structures that appear in the three-phonon calculation disappear in the six-phonon calculation. There is a tendency for the calculated distribution to split into two, one above and one below the barrier obtained in the no-coupling limit (NOC). The data, on the other hand, seem to favor a single, slightly asymmetric, broad barrier distribution.

It appears that the calculated cross sections have essentially converged with respect to multi-phonon excitations of the soft quadrupole mode in ^{100}Mo. The discrepancy with the data around 130 MeV could be due to transfer reactions or incomplete fusion. The discrepancy at the lowest energy is evidence of the fusion hindrance mentioned above. In fact, the *S* factor obtained from the data exhibits a maximum at about 121 MeV.[3]

[1]C. L. Jiang *et al.*, Phys. Rev. Lett. **93**, 012701 (2004).
[2]C. L. Jiang *et al.*, Phys. Rev. C **69**, 014604 (2004).
[3]C. L. Jiang *et al.*, Phys. Rev. C **71**, 044613 (2005).

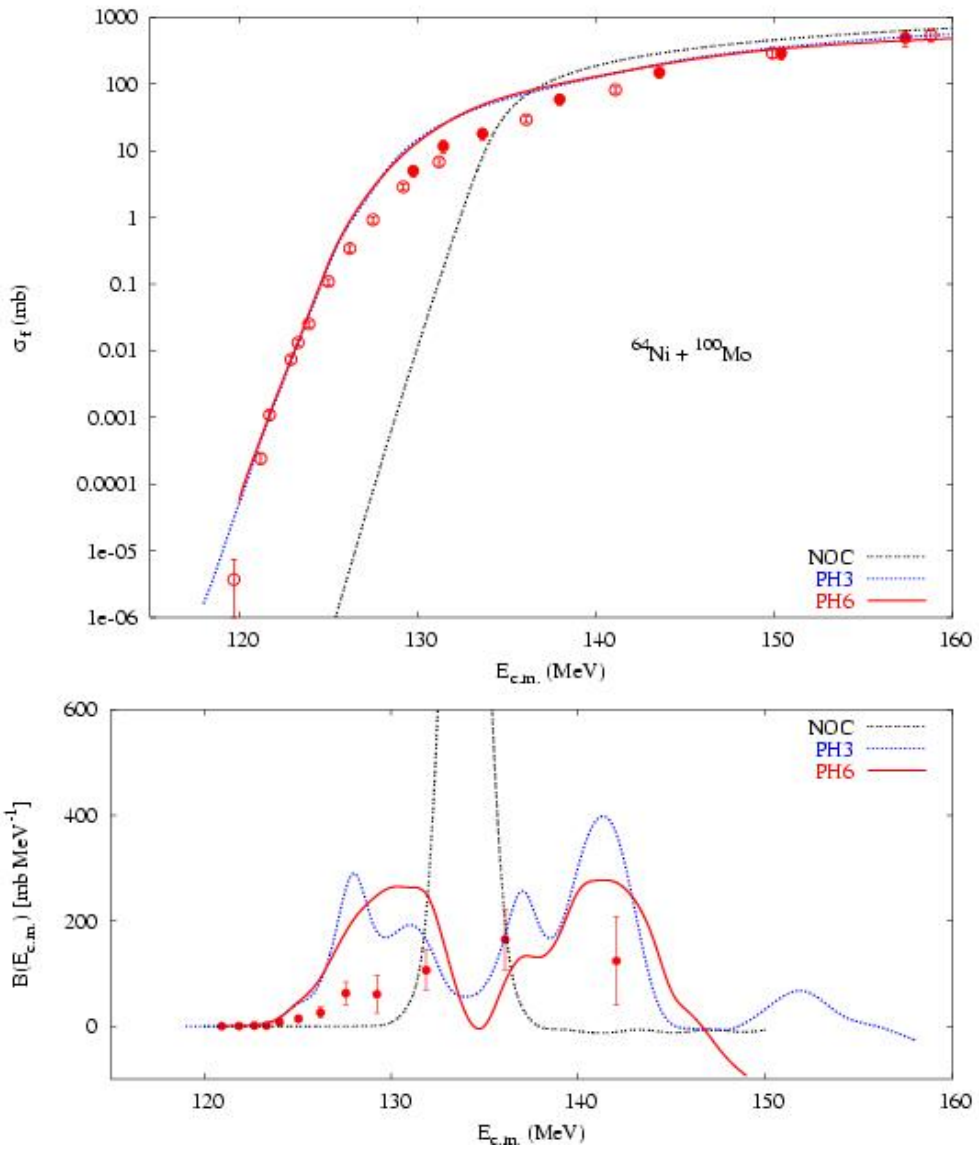

Fig. V-13. Fusion cross section for $^{64}Ni+^{100}Mo$ (top) and the associated barrier distribution (bottom). The data are from Ref. 3. The curves show the no-coupling limit (NOC), the three-phonon (PH3) and six-phonon (PH6) calculations described in the text.

d.2. Modeling the Quadrupole Mode in ^{100}Mo (H. Esbensen)

A problem in the application of the coupled-channels technique to heavy-ion fusion reactions is that the nuclear structure of the reacting nuclei is sometimes poorly known at or above the two-phonon level. It is therefore necessary to make model assumptions about the structure of higher lying states, in order to see their effect on fusion. The rotor and vibrator (harmonic oscillator) models are commonly used, but it would be very useful to have more flexible models that could be used to interpolate between these two extremes. One such model is the Bohr Hamiltonian, which in general depends on the deformation parameters (β,γ). This Hamiltonian is particularly easy to apply for γ-unstable nuclei, *i.e.*, when the potential of the Hamiltonian is independent of γ.

To illustrate the application of the Bohr Hamiltonian let us consider the ground state bands of three molybdenum isotopes. They are shown in the top part of Fig. V-14, where they have been normalized to one for the lowest 2^+

state. The red curves are the extreme rotor and vibrator models. The two black dashed curves are the spectra for the *E(5)* and *X(5)* dynamical symmetry models developed by Iachello.[1] The green curves are results for γ-unstable nuclei, which have been obtained numerically for the potential

$$V(\beta) = \frac{1}{2}(1-\eta)\beta^2 + \frac{\eta}{4}(1-\beta^2)^2$$

for the three values of the parameter η indicated in the figure. It is noted that the potential for $\eta = 0$ is the harmonic β^2 potential. The spectrum for ^{100}Mo is almost vibrational and it is reproduced quite well for $\eta = 1$.

The *B(E2)* values (normalized to one for the lowest transition) are shown in the bottom part of Fig. V-14. It is seen that the values for ^{100}Mo are only slightly above the green curve with $\eta = 1$. Thus it appears that the soft quadrupole mode in ^{100}Mo is described fairly well as a γ-unstable, slightly anharmonic vibration. Another feature that can be seen in the two figures is the good agreement between the model with $\eta = 5$ and the *E(5)* dynamical symmetry model. The reason for this is that the $\eta = 5$ potential resembles the square well potential that was used in the *E(5)* model.[1]

The model described above will be applied to calculate the matrix elements that are needed in coupled-channels calculations of heavy-ion fusion reactions of γ-unstable nuclei. The γ-stable nuclei, with $\gamma \approx 0$, is another simple limit that will be considered.

[1] F. Iachello, Phys. Rev. Lett. **85**, 3580 (2000); F. Iachello, Phy. Rev. Lett. **87**, 052502 (2001).

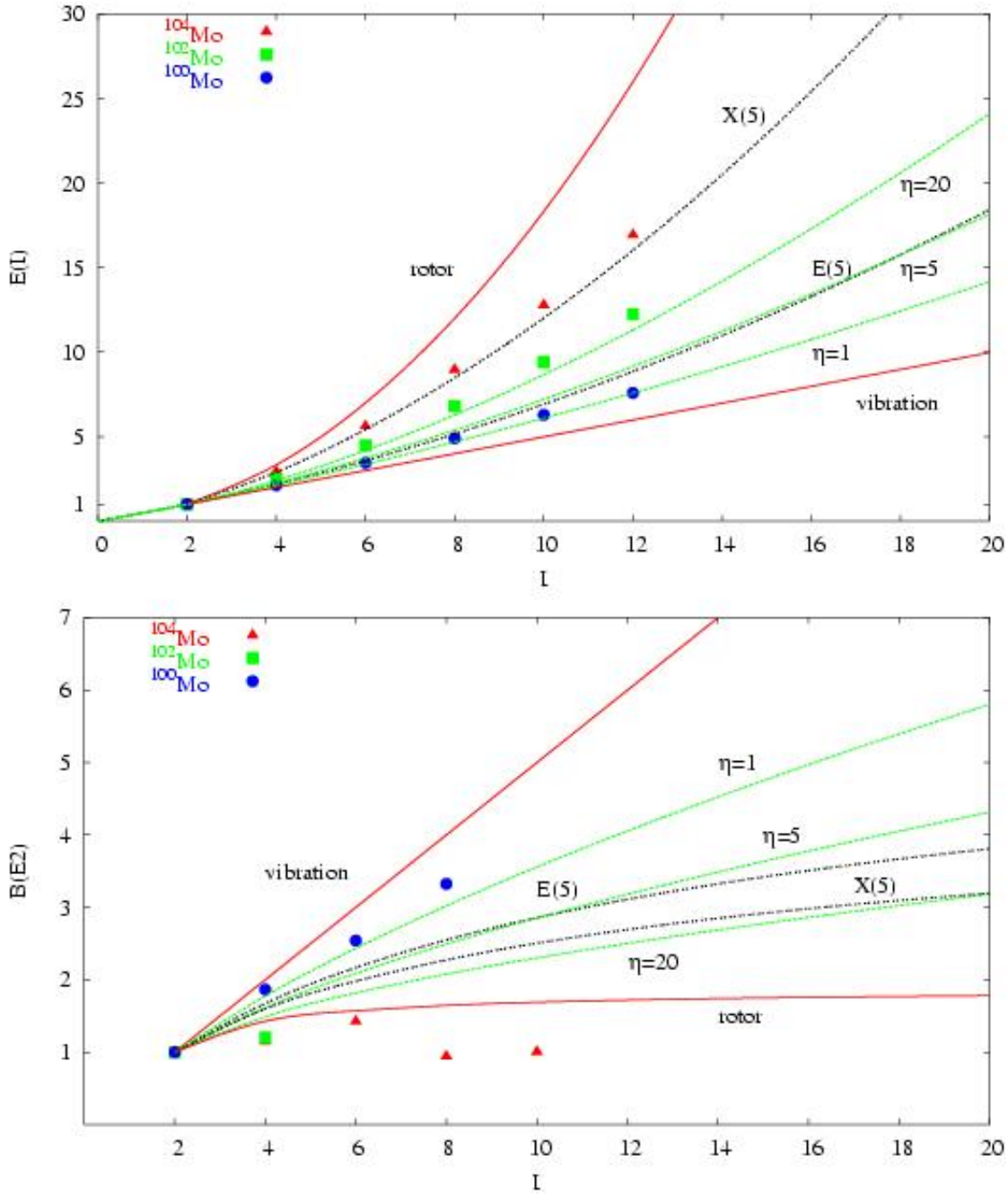

Fig. V-14. Ground state rotational bands of molybdenum isotopes (top part) and the associated B(E2) values (bottom part) are compared to different limits of the Bohr Hamiltonian.

d.3. Constraints on the $^{7}Be(p,\gamma)^{8}B$ Reaction from Charge Symmetry (H. Esbensen)

The cross section for the radiative proton capture on ^{7}Be is usually expressed in terms of the S factor at zero relative energy, $S_{17}(0)$. The recommended value[1] in 1998 was $S_{17}(0) = 19 \pm {}^{4}_{2}\ eV\ b$, and a large experimental effort has since gone into reducing the uncertainty. Unfortunately, the overlap between more recent results obtained with different techniques (radiative capture, Coulomb dissociation, transfer reactions) is still

marginal. It is therefore of interest to find other ways to put constraints on the ^8B *S* factor.

In a recent work[2] I assumed charge symmetry between ^8B and ^8Li and used the measured capture rate of thermal neutrons on ^7Li to predict the value of $S_{17}(0)$ for ^8B. The analysis was based on a simple two-body model of the valence proton (neutron) interacting with the ^7Be (^7Li) core. Calculations of the radiative capture rates were repeated for a wide range of the radius (2.1-2.9 fm) and the diffuseness (0.52-0.65 fm) of the nucleon-core nuclear potential, which was parametrized as a Woods-Saxon well. The depth for $p_{3/2}$ orbits was adjusted to give the correct separation energy. The depths for the *s*-waves (with total $J = 1^-$ and 2^-) were adjusted to reproduce the measured neutron scattering lengths on ^7Li.

The calculations were analyzed in terms of the asymptotic normalization constant *ANC*, which relates the asymptotic behavior of the ground state wave function $\varphi(r)$ to the Whittaker function, *i.e.*,

$$\varphi(r) = \frac{ANC}{r} W_{-\eta,l+1/2}(2\kappa r),$$

for large values of r. Here η is the Sommerfeld parameter, l is the orbital angular momentum, and κ is the wave number. The calculations showed a strong correlation between the capture rate and the *ANC*. For the proton capture one obtains

$$S_{17}(0) = 38.7\left[\text{eV b fm}\right]\left|\,\text{ANC}\left(^8\text{B}\right)\right|^2,$$

which is essentially independent of the radius and diffuseness of the nuclear potential. For the radiative neutron capture on ^7Li to the ground state of ^8Li one obtains the following relation between the measured[3] and calculated cross sections at thermal energy

$$N_{nc} = \frac{\sigma_{\text{expt}}}{\sigma_{\text{calc}}} = \frac{0.475 \pm 0.025 \pm 0.036\left(\text{fm}^{-1}\right)}{\left|\text{ANC}\left(^8\text{Li}\right)\right|^2}.$$

The first part of the uncertainty is due to the sensitivity to the parameters of the nuclear potential; the second part reflects the uncertainty in the measured neutron capture rate.[3]

One can interpret the quantity N_{nc} as a model-dependent spectroscopic factor. Assuming charge symmetry one can then apply the same spectroscopic factor to predict the *S* factor for ^8B. From the above relations one obtains the effective *S* factor,

$$S_{\text{eff}}(0) \approx N_{nc} \times S_{17}(0) = \left[18.4 \pm 1.0 \pm 1.4\left(\text{eV b}\right)\right]\left|\frac{\text{ANC}\left(^8\text{B}\right)}{\text{ANC}\left(^8\text{Li}\right)}\right|^2.$$

The ratio of the squares of the two ANC's is found to be 1.03 ± 0.02. The overall estimate is therefore $S_{\text{eff}}(0) \approx 18.9 \pm 1.8$ eV b, which is in very good agreement with the recommended value.[1]

It is noted that the conventional shell model approach cannot reproduce the ^8Li and ^8B capture data simultaneously. The main reason is that the shell model ground state of ^8Li (or ^8B) has at least two components, namely, a $p_{1/2}$ and a $p_{3/2}$ orbit of the valence nucleon, whereas the ground state is a pure $p_{3/2}$ orbit in the two-body model discussed above. This difference does not affect the ^8B capture rate but it causes the neutron capture rate on ^7Li to be about 25% higher in the shell model approach than in the two-body model, as explained in the publication.[2]

[1] E. G. Adelberger *et al.*, Rev. Mod. Phys. **70**, 1265 (1998).
[2] H. Esbensen, Phys. Rev. C **70**, 047603 (2004).
[3] J. E. Lynn, E. T. Jurney, and S. Raman, Phys. Rev. C **44**, 764 (1991).

d.4. Model Dependence of the ^{7}Be(p,γ)^{8}B Reaction Rate (H. Esbensen)

Measurements of the $^7Be(p,\gamma)^8B$ radiative capture cross sections are performed at relative energies of the proton and ^7Be, E_{rel}, that are much higher than the conditions inside the sun. In order to predict the capture rate at stellar conditions it is therefore necessary to extrapolate the measurements to low energy. This is done in terms of the *S* factor, $S_{17}(E_{rel})$, which has a rather modest energy dependence, but to make the extrapolation accurately it is necessary to rely on a good theoretical model for the energy dependence of the

S factor. A model that is sometimes preferred is a three-body model by Descouvemont and Baye from 1994, whereas two-body models are considered less reliable. Since a two-body model is much easier to use in reaction studies, it is of interest to see exactly where the two- and three-body models differ and by how much.

The energy dependence of the *S* factor for ^8B obtained in a two-body model[1] and in Descouvemont's most recent three-body model[2] are compared in Fig. V-15 with the recent capture data from Seattle.[3] Both calculations have been scaled so they agree with the data below 0.5 MeV. The dashed curves are the two-body results, which have been scaled by the factor 0.98; they show the contributions from *s*-wave and *d*-wave capture, and the sum. The nuclear radius and diffuseness of the two-body potential were set to 2.5 fm and 0.58 fm, respectively, and the depths were adjusted for each spin channel as described in Ref. 1. The solid red curves show the three-body results, which were obtained by multiplying Descouvemont's calculation[2] by a factor of 0.871. It is seen that the *d*-wave capture rates are essentially identical in the two models. The *s*-wave capture rates, on the other hand, start to differ at energies above 0.5 MeV.

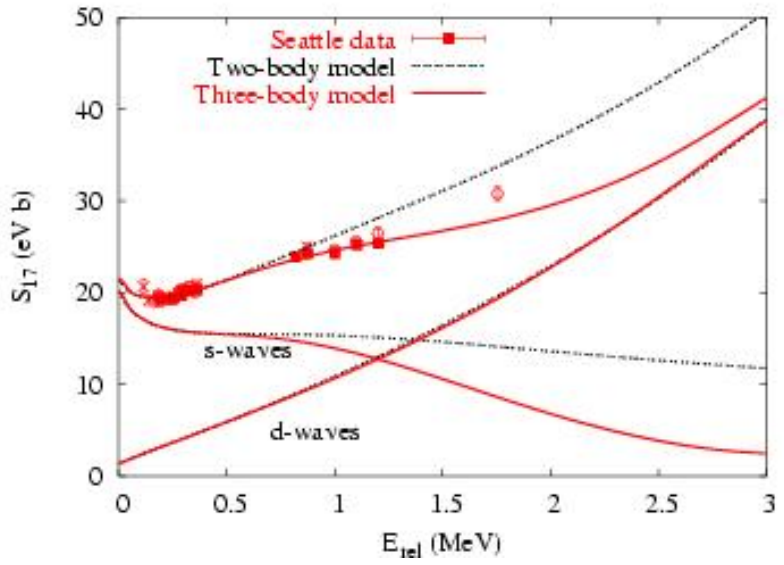

Fig. V-15. Measured[3] S factors for ^8B are compared to calculations based on a two-body[1] and a three-body model.[2] The separate contributions from s- and d-wave capture are also shown.

If the extrapolation of the measured *S* factors to zero relative energy is restricted to energies below the *M1* resonance, then the two- and three-body models should give the same value of $S_{17}(0)$, according to Fig. V-15. In fact, they both give $S_{17}(0) = 21.5$ eV b. The difference between the two models shows up at 1 MeV and higher energies, and it is seen that the three-body model is indeed favored by the Seattle data.[3]

[1]H. Esbensen, Phys. Rev. C **70**, 047603 (2004).
[2]P. Descouvemont, Phys. Rev. C **70**, 065802 (2004).
[3]A. R. Junghans *et al.*, Phys. Rev. C **68**, 065803 (2003).

d.5. Reconciling Coulomb Dissociation and Radiative Capture Measurements

(H. Esbensen, G. F. Bertsch,* and K. A. Snover*)

There is a significant discrepancy between the recent $^7Be(p,\gamma)^8$ radiative capture measurement[1] and the results extracted from measurements of the Coulomb dissociation (CD) of ^8B. The *S* factors extracted from the CD experiments are usually smaller, typically by 10-20% at low relative energies (E_{rel}) of the $^7Be + p$ final state, and the slope of the *S* factor is often steeper than obtained in the direct capture measurement. These

differences were identified and analyzed in detail in Ref. 1. They can also be seen in Fig. V-16 by comparing the results of two CD experiments[2,3] to the prediction of the three-body model (solid curve), which was calibrated in the previous section (see Fig. V-15) to reproduce the direct capture measurement.

In order to understand what causes the discrepancy between the direct and indirect measurements of the *S* factor for ^8B, we have examined the validity of the approximations that are commonly made in the analysis of CD experiments. The analysis is usually based on first-order perturbation theory and uses the so-called far-field (FF) approximations for the multipole expansion of the Coulomb field. Moreover, the analysis is often restricted to *E1* transitions. The FF approximation is based on the assumption that projectile and target do not overlap during the collision. We find that both the FF approximation and the first-order theory are inaccurate because of the weak binding and the extended density of the valence proton in ^8B.

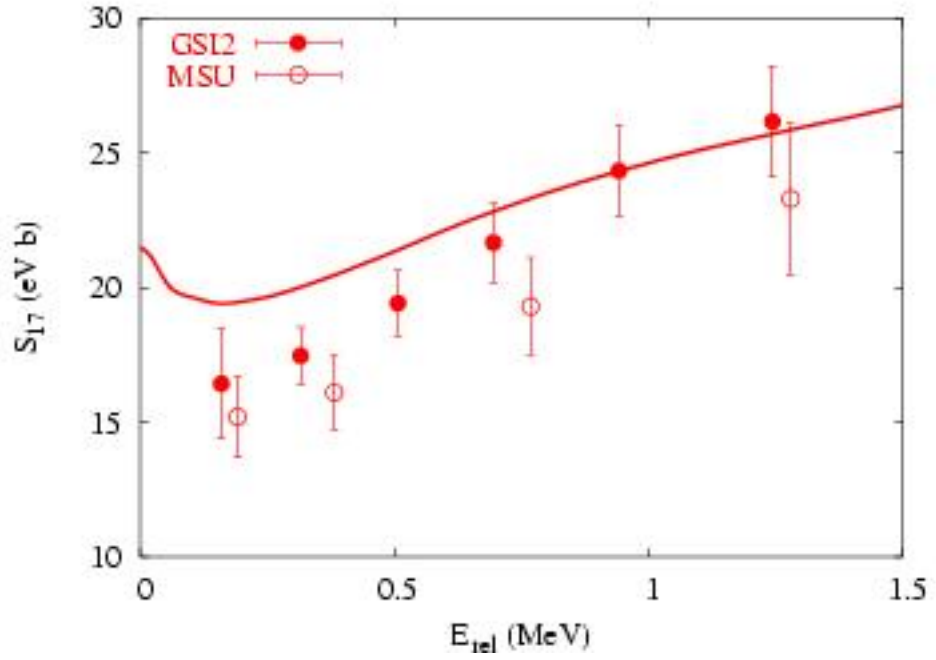

Fig. V-16. S factors for ^8B extracted from two Coulomb dissociation experiments[2,3] are compared to the result of the calibrated three-body model (solid curve), which reproduces the capture data in Fig. V-15.

We have used a semiclassical method to calculate the two-body breakup of ^8B into a proton and a ^7Be fragment.[4] This was done numerically by solving the time-dependent Schrödinger equation for the relative motion of the proton and the ^7Be core. The breakup is induced by the Coulomb and nuclear fields from a target nucleus, and the time-dependence is generated by the relative motion of projectile and target, which is assumed to follow a classical Coulomb trajectory.

The calculated decay energy spectra we obtain at 52 MeV/n and an impact parameter of 20 fm with a *Pb* target are shown in Fig. V-17. The top curve shows the result of first-order E1 + E2 transitions in the FF approximation, whereas the *E1* FF approximation is indicated separately by the solid points. The other curves show in decreasing order the effect of using the correct multipole form factors for the Coulomb field (instead of the FF approximation), of calculating the Coulomb dissociation to all orders (dynamic CD), and finally, the effect of also including the nuclear field from the target (dynamic CN). From the comparison of these calculations it is seen that *E2* transitions do have a significant strength in the first-order calculation, but their effect is accidentally compensated to some extent by the correct treatment of the Coulomb multipole fields and higher-order processes.

By comparing the solid points and the solid curve in Fig. V-17 it is seen that some discrepancy does remain between the conventional first-order *E1* calculation (solid points) and the full calculation (lowest solid curve). The full calculation is suppressed at low relative energies but it exceeds the conventional first-order *E1* calculation at

higher energies. These features provide a qualitative explanation of the observation that the *S* factors extracted from CD experiments are usually smaller at low relative energies and their slope is steeper than that obtained in the direct capture measurement. This work has been submitted for publication.[4]

*University of Washington.

[1]A. R. Junghans *et al.*, Phys. Rev. C **68**, 065803 (2003).
[2]F. Schüman *et al*., Phys. Rev. Lett. **90**, 232501 (2003).
[3]B. Davids *et al*., Phys. Rev. C **63**, 065806 (2001).
[4]H. Esbensen, G. F. Bertsch, and K. A. Snover, Phys. Rev. Lett. **94**, 0432502 (2005).

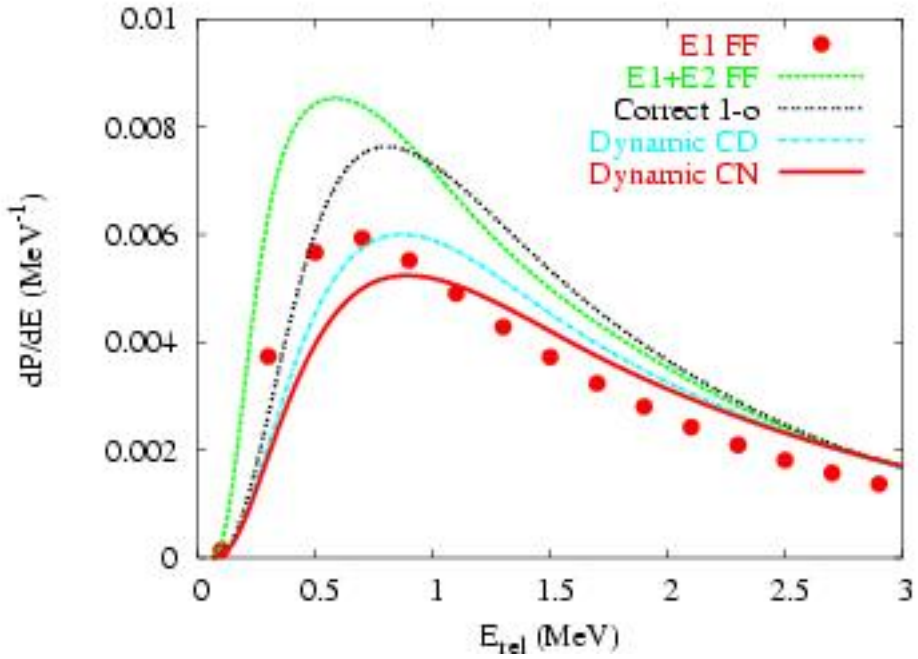

Fig. V-17. Decay energy spectrum for the dissociation of ^{8}B on Pb at 52 MeV/n and an impact parameter of 20 fm. The top curve shows the E1 + E2 FF approximation, and the solid points represent the commonly used E1 FF approximation. The other curves show in decreasing order the effect of using the correct Coulomb form factors to first order (Correct 1-o), of higher-order Coulomb processes (dynamic CD), and finally, the complete calculation which also includes nuclear couplings (dynamic CN).

d.6. Mean Field and Many Body Wave Functions (R. R. Chasman)

We are continuing the development of a program for calculating many-body variational wave functions that puts pairing and particle-hole two-body interactions on an equal footing. The complexity of the wave functions depends only on the number of levels included in the valence space. In these wave functions, we strictly conserve particle number and parity; projecting states of good particle number and parity before carrying out the variational calculations. We have extended the program to improve the treatment of neutron-proton pairing and have applied it to explain several features of nuclides near the $N = Z$ line. We have also improved the procedure for optimizing variational wave functions.

By using residual interaction strengths (*e.g.*, the quadrupole interaction strength or pairing interaction strength) as generator coordinates, one gets many different wave functions; each having a different expectation value for the relevant interaction mode. Such wave functions are particularly useful when one is dealing with a situation in which a configuration interaction treatment is needed. Because the same basis states are used in the construction of all the many-body wave

functions, it is possible to easily calculate overlaps and interaction matrix elements for the many-body wave functions obtained from different values of the generator coordinates (which are not in general orthogonal). The valence space can contain a very large number of single-particle basis states, when there are constants of motion that can be used to break the levels up into sub-groups. To increase the manageable size of the valence space, we have parallelized our code to run on the jazz computer system, and we are modifying the code to deal with octupole correlations in heavy nuclei. We have used the generator coordinate method to calculate configuration interaction admixtures for the *n-p* pairing wave functions. This is important for calculating pair transfer transition probabilities.

d.7. Neutron-Proton Pairing (R. R. Chasman)

We have developed[1-3] a treatment of neutron-proton pairing that explains many features of nuclear structure seen near the $N = Z$ line. Our many-body treatment includes *n-p* pairing, as well as like particle pairing, with full projection of neutron and proton particle number before doing a variational calculation. We also found that there is a new quantum number that holds exactly for collective states; *i.e.*, those states in which no levels are blocked. This new quantum number (Q) is the number parity of the $T = 0$ and $T = 1$ *n-p* pairs. Fixing the number parity of one *n-p* mode fixes the other, because we conserve proton number and neutron number exactly. This number parity is closely related to the isospin quantum number. These collective states are the ground states for $N = Z$ nuclides. We project Q before doing a variational calculation. The form of our variational wave function includes an explicit amplitude for "alpha like" correlations in each level as well as the usual amplitudes for *n-n*, *p-p* and *n-p* pairs. We have added terms to the *n-p* pairing interaction that allow pairs of particles in the same orbitals, giving states with maximum angular momentum. Because of the exclusion principle, these must be *n-p* pairs and $T = 0$.

In odd-odd $N = Z$ nuclei, the ground state is a degenerate doublet, consisting of a $Q = 0$ and $Q = 1$ state, when the $T = 0$ and $T = 1$ pairing strengths are equal. The splitting of this ground state doublet affords some information about the relative strengths of the $T = 0$ and $T = 1$ pairing strengths. In even-even nuclei, there is a large splitting between the 0^+ $T = 1$ ground state and the 1^+ $T = 0$ excited state. Our model explains this feature in a transparent way. Most of the excitation energy owes to the breaking of a quartet and the single particle excitation energy involved in making a $T = 0$ pair. In the odd-odd $N = Z$ nuclei case, neither of these effects applies for the $T = 0$ state.

The Wigner energy is the extra binding energy of $N = Z$ even-even nuclei relative to neighboring nuclei. Our approach explains the magnitude of the Wigner energy very well. It owes to the extra pairing energy involved in creating a quartet of nucleons in the same orbital.

Our detailed calculations of the dependence of the binding energies on the relative strengths of the $T = 0$ and $T = 1$ pairing strengths shows that the differences are small as a function of the variation of the relative strengths. Other observables are needed to establish the magnitude of $T = 0$ correlations in nuclei. To that end, we have carried out a calculation of the *n-p* pair transfer spectroscopic factor. In our calculation, the initial state is an even-even $N = Z$ nuclide and the final states are the lowest $T = 1$ and $T = 0$ states in the neighboring odd-odd $(Z+1,N+1)$ nucleus. The relative spectroscopic factors show a considerable sensitivity to the relative strengths of the $T = 0$ and $T = 1$ pairing strengths. A 20% reduction of the $T = 0$ pairing strength gives a 40% reduction in the ratios of $T = 0/T = 1$ pair transfer probabilities. In Fig. V-18, we show single particle levels that are appropriate for the ^{56}Ni region. The blue levels are taken from a Woods-Saxon calculation and the red levels have been shifted to give level spacings in agreement with experimental data. In Fig. V-19, we show the pair transfer probability to the lowest lying $T = 0$ and $T = 1$ states in ^{58}Cu, as a function of $T = 0$ pairing strength, keeping the $T = 1$ pairing strength fixed. The interaction is semi-realistic in this calculation, as we use constant matrix elements for each of the pairing modes.

[1] R. R. Chasman, Phys. Lett. **B524**, 81 (2002).
[2] R. R. Chasman, Phys. Lett. **B553**, 204 (2003).
[3] R. R. Chasman, Phys. Lett. **B577**, 47 (2003).

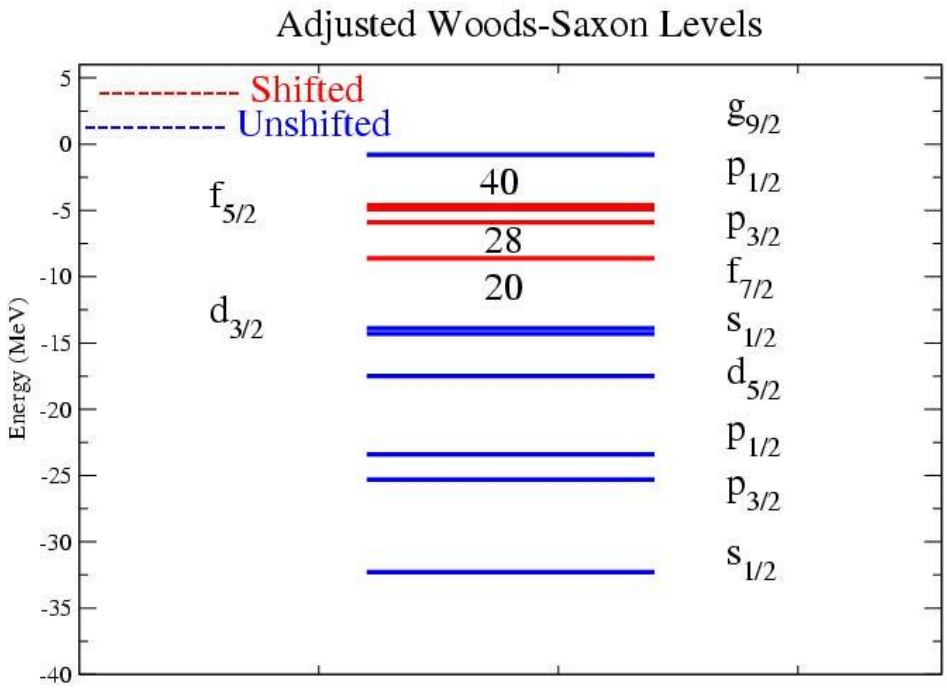

Fig. V-18. Single-Particle States of ^{56}Ni used in calculating pair transfer probability. The states shown in blue are taken directly from a Woods-Saxon calculation. The states shown in red are adjusted to get agreement with level spacings that have been determined experimentally.

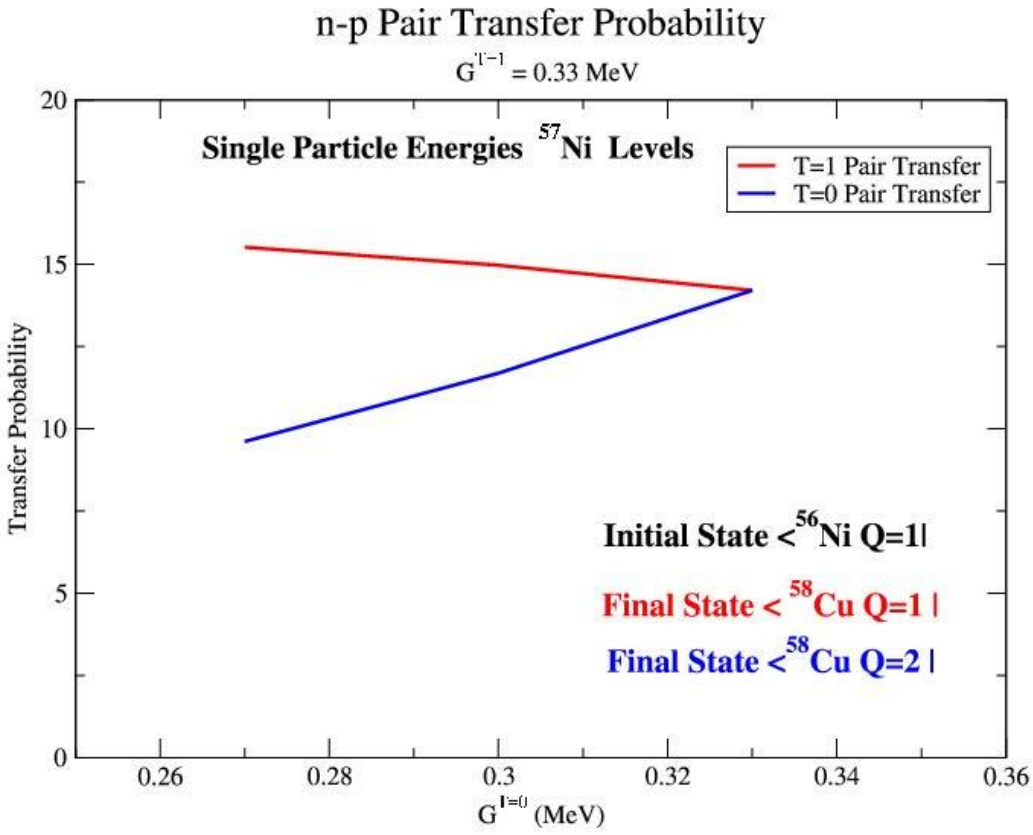

Fig. V-19. Pair Transfer Spectroscopic Factors. The spectroscopic factors are shown for N-P pair transfer to levels in ^{58}Cu from the ground state of ^{56}Ni, as a function of T = 0 pairing interaction strength. The T = 1 pairing strength is held constant. Semi-realistic matrix elements were used in this calculation.

d.8. Energy Levels of the Heavy Elements (I. Ahmad, and R. R. Chasman)

The study of single-particle states in the heavy elements is a long-term collaborative project. The low-lying states in odd-mass nuclides provide a good test of the parametrizations of single particle models. Vibrational admixtures are usually small for these states. The single-particle energy level spacings in the heavy elements provide useful guidance for single-particle potentials that are appropriate for super-heavy elements. Seven single-particle states have been identified[1] in ^{247}*Cm*, so this nuclide provides a particularly good test of neutron single particle potentials. Eight single-particle levels have been identified[2] in ^{249}*Bk*. This provides a very good test of proton single-particle potentials in the very heavy elements. When pairing effects are extracted from the observed levels in ^{247}*Cm* and ^{249}*Bk*, the orderings and spacings of levels are in good agreement with the levels obtained from our parametrization of a deformed Woods-Saxon potential. These analyses will provide useful constraints on other parametrizations of superheavy potentials. In Fig. V-20, we display the comparison of single-particle levels of ^{249}*Bk* extracted from experiment with a density-dependent-delta interaction[3] and single-particle spacings obtained from a Woods-Saxon potential.

[1] I. Ahmad *et al*., Phys. Rev. C **68**, 044306 (2003).
[2] I. Ahmad *et al*., Phys. Rev. C **71**, 054305 (2005).
[3] R. R. Chasman, Phys. Rev. C **14,** 1935 (1976).

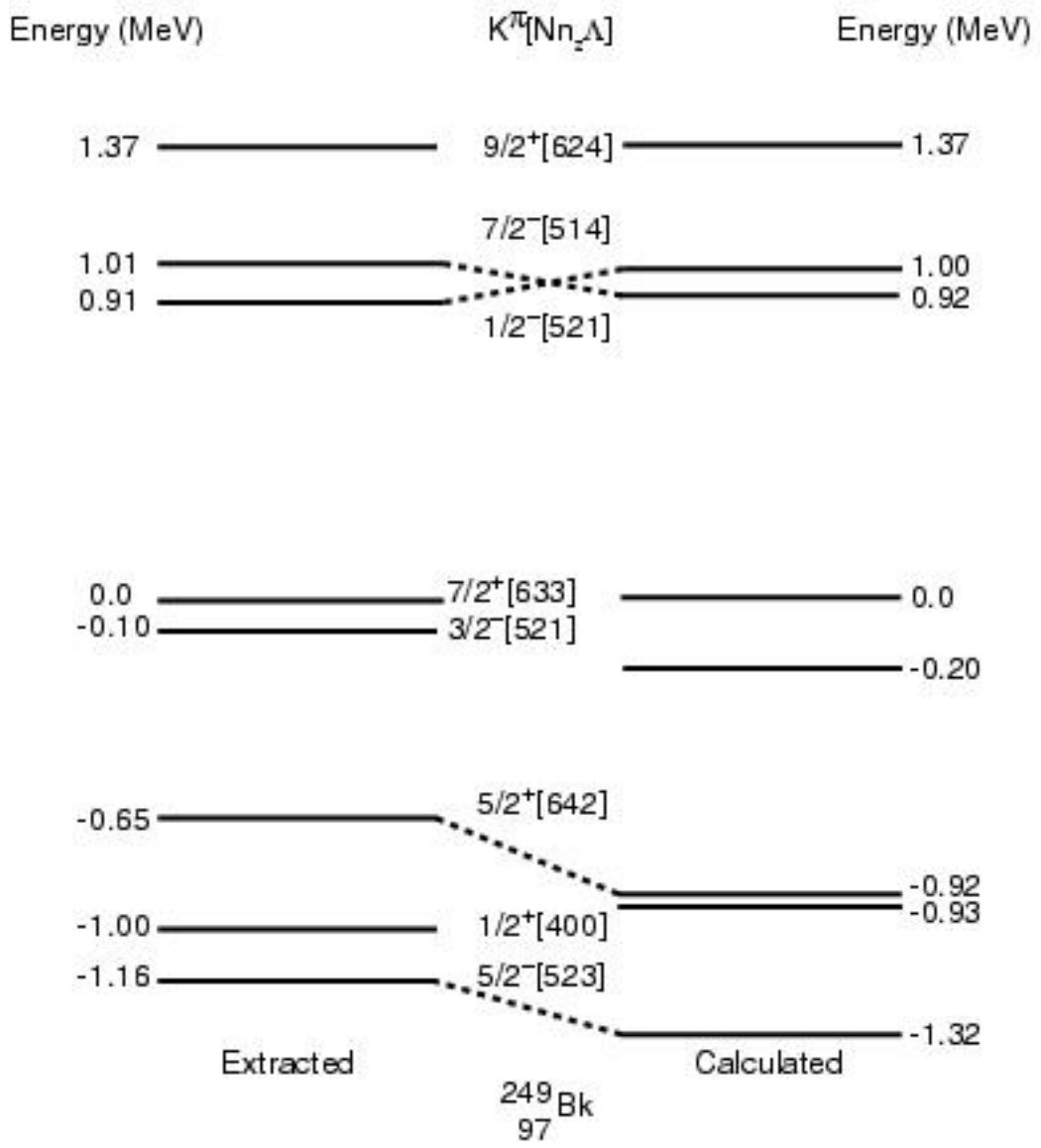

Fig. V-20. Comparison of calculated and observed energy single particle level spacings in ^{249}Bk. The extracted levels are obtained from experimental data by removing pairing effects from experiment. The calculated levels were obtained from a Woods-Saxon potential having deformation parameters $v_2 = 0.255$, $v_4 = 0.01$ and $v_6 = 0.015$.

d.9. Self-Consistent Beyond-Mean-Field Calculations in Exotic Heavy Nuclei

(T. Duguet, M. Bender,* P.-H. Heenen,† and P. Bonche‡)

We studied the low-lying collective excitation spectra of the neutron-deficient lead isotopes ^{182}*Pb*-^{194}*Pb* by performing a configuration mixing of angular-momentum and particle-number projected self-consistent mean-field states. This study supported the interpretation of spectra made on the grounds of more schematic models in terms of coexisting spherical, oblate, prolate and superdeformed prolate structures. Theoretical spectra and transition probabilities (*E0* and *E2*) are in relatively good agreement with experimental data. We predicted the presence of superdeformed bands at low excitation energy in the most neutron-deficient isotopes. A paper describing this work was published.[1]

*University of Washington, †Universite Libre de Bruxelles, Belgium, ‡Commissariat a L'Energie Atomique, Saclay, France.
[1]M. Bender, P. Bonche, T. Duguet, and P.-H. Heenen, Phys. Rev. C **69**, 064303 (2004).

d.10. A New Microscopic Pairing Force for Self-Consistent Mean-Field Calculations (T. Duguet)

We derived a microscopic finite-range effective pairing force from the bare nucleon-nucleon interaction. It reproduces exactly the pairing provided in infinite matter by the AV18 *NN* interaction. By going from the bare to a well-defined effective force explicitly, we disentangled the effects of the range and of the density dependence of the effective pairing interaction. In particular, the relative success of existing phenomenological finite-range/density-independent and zero-range/density-dependent forces could be explained on a more fundamental basis. The interaction was made simple enough to be used in self-consistent mean-field calculations of finite nuclei. The first three-dimensional HFB calculations using this new microscopic interaction were carried out and led to a conference proceedings publication.[1] These first calculations confirmed the crucial isovector and low density character of the force when predicting properties of neutron rich nuclei.

[1]T. Duguet and P. Bonche, AIP Conference Proceedings **764**, 277 (2005).

d.11. Configuration Mixing of Particle-Number and Angular-Momentum Projected Cranked HFB States (M. Bender and P.-H. Heenen*)

Self-consistent mean-field models are one of the standard approaches in nuclear structure theory. For heavy nuclei, they are the only fully microscopic method that can be systematically applied on a large scale. Despite its many successes, the mean-field approach has several shortcomings and limitations. Including correlations associated with fluctuations of collective degrees of freedom into the modeling via the framework of the projected Generator Coordinate Method removes many of these deficiencies, and simultaneously gives access to shape mixing and collective excitation modes.

Our existing method for configuration mixing of particle-number and angular-momentum projected axially symmetric and time-reversal invariant mean-field states, which has successfully been applied to nuclei throughout the chart of nuclei[1] was generalized to use cranked triaxial HFB states as the starting point. This allows an extension of the calculations to the whole β-γ plane of quadrupole deformations, and to incorporate effects from the alignment of single-particle states. Several theoretical problems regarding the use of the remaining symmetries, relative phases, and the transformations between various bases of HFB theory were solved to obtain a numerically efficient code. From the generalized model we expect an improvement of the excitation energies, which were systematically slightly too high in the existing model. First results from test calculations for light nuclei are encouraging.

*Universite Libre de Bruxelles, Belgium.
[1]M. Bender and P.-H. Heenen, Eur. Phys. J. A **25**, 519 (2005).

d.12. Collective States in the $20 < Z < 28$ and $28 < N < 40$ Region (M. Bender and P.-H. Heenen*)

A systematic study of the collective quadrupole excitations of the nuclei with $20 < Z < 28$ and $28 < N < 40$ was performed in the framework of configuration mixing of particle-number and angular-momentum projected self-consistent axial mean-field states. This region of the chart of nuclei is of current interest as the excitation spectra around ^{54}Ti and ^{56}Ti show anomalies, which are often associated with enhanced

(sub-)shell closures at $N = 32$ and $N = 34$.[1,2] With our method we obtain fair agreement between calculations and the available experimental data for excitation energies and transition moments without having strong $N = 32$ and $N = 34$ sub-shell closures. Further analysis is underway.

*Universite Libre de Bruxelles, Belgium.
[1]S. N. Liddick *et al.*, Phys. Rev. C **70**, 064303 (2004).
[2]B. Fornal *et al.*, Phys. Rev. C **70**, 064304 (2004).

d.13. Systematics of Ground-State Correlations in Even-Even Nuclei (M. Bender, G. F. Bertsch,* and P.-H. Heenen†)

Ground-state correlations beyond the mean-field are a key element of successful microscopic mass formulae. We studied the correlation energies associated with the quadrupole shape degrees of freedom with a view to improving the self-consistent mean-field theory of nuclear binding energies. Systematic calculations were performed for more than 600 even-even nuclei from mass number 16 up to superheavy ones,[1] using the Skyrme interaction SLy4 in connection with a density-dependent pairing interaction and the angular-momentum projected generator coordinate method. The quadrupole correlation energies range from 0.5 to 6.0 MeV, and their inclusion improves two qualitative deficiencies of the mean-field theory; namely, the exaggerated shell effect at neutron magic numbers and the failure of mean-field theory to describe mutually enhanced magicity. For the mass table as a whole, the quadrupolar correlations improve binding energies, separation energies, and separation energy differences by 20%-30%.

*University of Washington, †Universite Libre de Bruxelles, Belgium.
[1]M. Bender and P.-H. Heenen, Eur. Phys. J. A **25**, 519 (2005).

d.14. QRPA of Spherical Nuclei with Skyrme Interactions (M. Bender, J. Terasaki,* J. Engel,* J. Dobaczewski,† W. Nazarewicz,† and M. Stoitsov†)

We developed[1] the first fully self-consistent implementation of a quasiparticle random-phase approximation (QRPA) for arbitrary Skyrme energy density functionals and density-dependent pairing functionals. We use the canonical Hartree-Fock-Bogoliubov basis for the numerical representation of the QRPA equations. The goal of the approach is to accurately describe multipole strength functions in spherical even-even nuclei, including weakly bound drip-line systems. The accuracy of the method was carefully tested, particularly in handling spurious modes. We also investigated the consequences of neglecting the spin-orbit or Coulomb residual interactions in the QRPA, a common practice in the literature so far. First calculations were performed for isoscalar and isovector monopole, dipole, and quadrupole strength functions in several *Sn* isotopes, both in the stable region and at the drip lines.

*University of North Carolina, †Oak Ridge National Laboatory and University of Tennessee.
[1]J. Terasaki, J. Engel, M. Bender, J. Dobaczewski, W. Nazarewicz, and M. Stoitsov, Phys. Rev. C **71**, 034310 (2005).

E. ATOMIC THEORY AND FUNDAMENTAL QUANTUM MECHANICS

In addition to research on hadronic and nuclear physics, and nuclear astrophysics, we also conduct research in atomic physics, neutron physics, and quantum computing.

Work in atomic physics includes the studies of interactions of electrons or high-energy photons with matter, in support of experiments performed at Argonne's Advanced Photon Source (APS). Theoretical studies are being conducted on the physics of the photoeffect and Compton scattering by bound electrons, focusing on topics selected in view of basic importance, timeliness, and potential in applications. Comprehensive surveys of photo-interaction data for silicon and graphite are underway.

Theoretical work in support of a new experiment to measure the neutron electric-dipole moment continues. This experiment will be conducted at NIST. A proof-of-principle experiment to measure the neutron magnetic-dipole moment in the same way has been approved for the Missouri University Research Reactor. Most of the needed equipment has been built. In addition, work continues to extend the spin-statistics theorem in nonrelativistic quantum mechanics to particles with non-zero spins.

Work continued toward the development of a coherent theory of physics and mathematics. One approach aims to replace the complex number field C, used as the base for the mathematical structures of a physical theory, by the numbers in $C_n = (R_n, I_n)$. The positive real number component R_n corresponds to the infinite discrete hierarchy of binary numbers $\underline{s} \times 2^{n(2e-1)}$ where $\underline{s}$ is a length n 0-1 sequence and e is any integer. R_n is based on the properties of outputs from an infinite hierarchy of binary measurement outputs of length n for any continuous variable with an infinite range. This work emphasized the properties of a discrete space, S_n, based on these numbers. The exponential scale independence of S_n showed the presence of singularities or accumulation points at any coordinate system origin and on coordinate axes. The possible usefulness of S_n to describe inflationary cosmology was developed. The big bang, inflation, and recovery of a discrete space time that is empirically indistinguishable from a continuum space time is obtained by making $n = n(t)$ and $e = e(t)$ depend on cosmological time t. The Hubble expansion is also included. While no physical model was developed to justify the time dependence, it was made apparent that these aspects of cosmological dynamics can easily be accommodated in S_n.

e.1. Interactions of Photons with Matter (M. Inokuti and D. Y. Smith*)

In support of experiments in atomic and condensed-matter physics with the use of synchrotron radiation, theoretical studies are being conducted on the physics of photo-absorption and Compton scattering, focusing on topics selected in view of basic importance, timeliness, and potential applications.

One theme of long-term studies has been the use of dispersion relations and sum rules for indices of response of matter over the entire range of photon energies. A comprehensive analysis of optical data on silicon is nearly complete. As an application, the data permit us to evaluate the mean excitation energy I in the Bethe stopping-power formula. The best set of data in our present judgment gives $I = 163.5 \pm 2$ eV, appreciably lower than the current standard value, 173 ± 3 eV.

An analysis of reflectivity and absorption of silicate glasses has led to good understanding of the role of disorder and modifier ions in determining the refractive index for visible light.[1]

*University of Vermont.

[1]D. Y. Smith, E. Shiles, and M. Inokuti, Phys. Stat. Sol. (c) **2**, 310 (2005).

e.2. Interactions of Charged Particles with Matter (M. Inokuti)

Stopping power, the total yield of ionization, and its statistical fluctuations are examples of quantities describing the penetration of charged particles through matter and are important to applications such as the detection of particles and the analysis of their charges and kinetic energies. The understanding of those quantities in terms of individual collisions and associated cross sections remains a major challenge and is the goal of our continuing effort. Current work is the evaluation of the mean excitation energies, namely, the *I* values, in the Bethe stopping-power formula from the oscillator-strength spectra for nine atoms and 23 molecules that are treated by Berkowitz.[1] Results were reported at an international meeting.[2]

Extensive work for the International Commission on Radiation Units and Measurements (ICRU) continues on the editing of its reports and on physical data such as stopping powers and various interaction cross sections.

[1]J. Berkowitz, Atomic and Molecular Photoabsorption. Absolute Total Cross Sections (Academic Press 2002).
[2]S. Kamakura, N. Sakamoto, H. Ogawa, H. Tsuchida, and M. Inokuti, in Program and Abstracts, "Fourth International Conference on Atomic and Molecular Data and Their Applications," October 5-8, 2004, Toki, Japan (National Institute for Fusion Science, 2004), p. 64.

e.3. Photon Beam Polarization and Non-Dipolar Angular Distributions (N. K. Meshkov and M. Peshkin)

We are updating earlier work, some unpublished, on the consequences of spatial symmetries for the angular distributions of photons scattered by, and of electrons ejected from, atoms and molecules irradiated by polarized photon beams. The purpose of this analysis is to identify the dynamical parameters that can be extracted from measured angular distributions under conditions where the polarization is accurately known and controlled and also under conditions where the polarization is not known. Because the earlier results have proved to be useful to experimenters in the design of experiments and in the analysis of experimental data, we are now extending them and preparing them for publication.

e.4. The Theory Experiment Connection: R_n Space and Inflationary Cosmology[1] (P. Benioff)

Earlier work[2,3] on the theory-experiment connection and R_n space was continued with emphasis on the properties of R_n space and its use to describe the big bang and inflation in cosmology. The basic idea starts with the observation that all physical theories are mathematical structures over R and C, the real and complex numbers where R is part of C. Also space and time inherit the continuum properties of R. Here R is replaced with R_n which is the set of numbers of the binary form $s.t \times 2^{2ne}$ where s and t are functions from the interval 1,2,….,n to {0,1} and e is any integer. This form is based on the observation that all measurements of quantities with an infinite range (*e.g.*, distance) have this form as the number of significant figures is almost independent of the magnitude of the measurement.

R_n space is based on these numbers. Each dimension is discrete and consists of an infinite number of regions separated by exponential jumps. Each region contains $2^{2n}-1$ points with adjacent points separated by a distance $0_{[1,n]}.0_{[1,n-1]}1 \times 2^{2ne}$. Adjacent regions are separated by exponential jumps with e going to $e + 1$. The origin of

any coordinate system is a point of accumulation or space singularity.

R_n space was shown to be a natural arena to describe the big bang and inflation. The idea is to make n and e depend on cosmological time τ as $n = n(\tau)$ and $e = e(\tau)$. At $\tau = 0$ e is required to be $\leq e_0$, a negative integer, and $n(0)$ small, around 10. This crams all of space into a ball of radius $2^{n(0)(2e_0+1)}$. As τ increases $R_n(\tau)$ space expands at a constant rate of one step per time interval Δ. The expansion velocity is constant at $2^{n(2e-1)}/\Delta$ for $2^{2n}-1$ steps followed by an exponential jump to a higher velocity of $2^{n(2(e+1)-1)}/\Delta$, for another $2^{2n}-1$ steps, etc. This expansion increases spatial distances at an exponential rate when averaged over 2^n steps. This gives an inflation. When the outer regions of R_n space are expanding at velocities $> c$, inflation is stopped at some time τ' by having $n(\tau)$ increase from some value around 10 to a value of 100 or more. The resulting space region for $e = 0$ is experimentally indistinguishable from ordinary continuum space as the points are separated by at most the Planck length and the region diameter is greater than the size of the observable universe. Hubble expansion is also easily included. This shows that R_n space is not implausible, even though no physical derivation of the time dependence of n and e is provided.

[1]P. Benioff, in "Proceedings of SPIE, Vol. 5833: Quantum Informatics 2004", ed. Yu. I. Ozhigov (SPIE, Bellingham, WA, 2005) 1.
[2]P. Benioff, Foundations of Physics **35**, 1825 (2005).
[3]P. Benioff, in "Proceedings of SPIE, Vol. 5833: Quantum Informatics 2004", ed. Yu. I. Ozhigov (SPIE, Bellingham, WA, 2005) 1.

F. OTHER ACTIVITIES

f.1. Hadron Physics: Modern Methods for Modern Challenges (A. Höll, A. Krassnigg, and C. D. Roberts)

We secured funding from the Argonne Theory Institute (http://www.anl.gov/ati/) to run a Theory visitor program, which brought together experts focused on the modern tools of hadron physics: Dyson-Schwinger equations (DSEs); lattice-regularized quantum chromodynamics (LQCD); light-front quantum field theory; QCD modeling; and relativistic quantum mechanics, to identify promising methods for meeting the theoretical challenges that a 12 GeV upgrade of the CEBAF at JLab will provide. Visitors were invited to ANL to speak, and discuss the merits of their chosen research tools. Results were compared and opportunities for constructive feedback explored. The discussions led to significant improvements in our understanding of the role played by the quark-gluon vertex in QCD's gap equation. In addition, a connection was built between JLab's lattice group and DSE practitioners in Ohio and Pennsylvania, with the latter undertaking to study the current-quark mass dependence of hadron observables that is not accessible to current lattice simulations; and lattice-QCD practitioners were challenged to verify numerically new and exact results in QCD proved by DSE methods. Discussions were also held on the role and nature of diquark correlations in exotic baryons. One particular success was the identification of a means by which a useful model of the dressed-quark-gluon vertex could be constructed from a Slavnov-Taylor identity. This simple model was later employed to explore the validity of lattice data on this Schwinger function, with the result that the lattice-inferred form of one subdominant amplitude is very likely erroneous.

f.2. 17th Annual Midwest Theory Get-Together (C. D. Roberts)

The Theory Group hosted the seventeenth Annual Midwest Theory Get-Together on September 24-25, 2004. Nuclear theorists from eight Midwest universities and ANL met to learn about the research goals and foci of different individuals and groups throughout the region. While the organizational duties rotate amongst the participants, Argonne is the regular host site because of its meeting facilities and central location. The organizers for 2004 were William Klink and Wayne Polyzou from the University of Iowa in Iowa City. The meeting provides a good chance for students to broaden their outlook and get some practical speaking experience in a friendly atmosphere. The format is informal, with an agenda of talks being volunteered at the beginning of the meeting. In 2004 we had thirty registered participants: faculty, postdocs and students. Over the Friday afternoon and Saturday morning approximately twenty-five presentations were made, covering topics such as: effective field theories; hadron physics and QCD; the nuclear shell model, nuclear pairing and nucleon matter; quantum Monte-Carlo methods; relativistic heavy ion collisions; and relativistic quantum mechanics for few body systems. It was a successful event.